

# Lagrangian analysis of moisture sources of Tianshan Mountain precipitation

Xuefeng Guan<sup>1</sup>, Lukas Langhamer<sup>2</sup>, and Christoph Schneider<sup>2</sup>

<sup>1</sup>Humboldt-Universität zu Berlin, Germany

<sup>2</sup>Humboldt-Universität zu Berlin

November 18, 2022

## Abstract

The moisture sources of precipitation in the Tianshan Mountains, one of the regions with the highest precipitation in Central Asia during 1979-2017 are comprehensively and quantitatively summarized by using a Lagrangian moisture source detection technique. Continental sources provide about 93.2\% of the moisture for precipitation in the Tianshan Mountain, while moisture directly from the ocean is very limited, averaging only 6.8\%. Central Asia plays a dominant role in providing moisture for all sub-regions of the Tianshan Mountains. For the Western Tianshan, moisture from April to October comes mainly from Central Asia (41.4\%), while moisture from November to March is derived primarily from Western Asia (45.7\%). Nearly 13.0\% of moisture to precipitation for Eastern Tianshan in summer originates from East and South Asia, and the Siberia region. There is a significant decreasing trend in the moisture contribution of local evaporation and Central Asia in the Eastern Tianshan during winter. The contribution of moisture from Europe to summer precipitation in the Central and Eastern Tianshan and the contribution of the North Atlantic Ocean to summer precipitation in the Northern, Central, and Eastern Tianshan also exhibit a decreasing trend. The largest increase in moisture in Western Tianshan stems from West Asia during extreme winter precipitation months. Europe is also an important contributor to extreme precipitation in the Northern Tianshan. The moisture from East and South Asia and Siberia during extreme precipitation months in both winter and summer is significantly enhanced in the Eastern Tianshan.

# Lagrangian analysis of moisture sources of Tianshan Mountain precipitation

Xuefeng Guan, Lukas Langhamer, Christoph Schneider

Geography Department, Humboldt-Universität zu Berlin, Berlin, Germany

## Key Points:

- A Lagrangian moisture source detection technique is applied to reveal the moisture sources of precipitation in the Tianshan Mountains.
- Local evaporation and Central Asia play a leading role in providing moisture for all sub-regions of the Tianshan Mountains.
- The moisture from East and South Asia (ESA) and Siberia during extreme precipitation months is significantly enhanced in the Eastern Tianshan.

---

Corresponding author: Xuefeng Guan, [xuefengg@geo.hu-berlin.de](mailto:xuefengg@geo.hu-berlin.de)

**Abstract**

The moisture sources of precipitation in the Tianshan Mountains, one of the regions with the highest precipitation in Central Asia during 1979-2017 are comprehensively and quantitatively summarized by using a Lagrangian moisture source detection technique. Continental sources provide about 93.2% of the moisture for precipitation in the Tianshan Mountain, while moisture directly from the ocean is very limited, averaging only 6.8%. Central Asia plays a dominant role in providing moisture for all sub-regions of the Tianshan Mountains. For the Western Tianshan, moisture from April to October comes mainly from Central Asia (41.4%), while moisture from November to March is derived primarily from Western Asia (45.7%). Nearly 13.0% of moisture to precipitation for Eastern Tianshan in summer originates from East and South Asia, and the Siberia region. There is a significant decreasing trend in the moisture contribution of local evaporation and Central Asia in the Eastern Tianshan during winter. The contribution of moisture from Europe to summer precipitation in the Central and Eastern Tianshan and the contribution of the North Atlantic Ocean to summer precipitation in the Northern, Central, and Eastern Tianshan also exhibit a decreasing trend. The largest increase in moisture in Western Tianshan stems from West Asia during extreme winter precipitation months. Europe is also an important contributor to extreme precipitation in the Northern Tianshan. The moisture from East and South Asia and Siberia during extreme precipitation months in both winter and summer is significantly enhanced in the Eastern Tianshan.

**1 Introduction**

The Tianshan mountains form a prominent so-called water tower in Central Asia providing major parts of the water resources of the surrounding lowlands (Immerzeel & Bierkens, 2012; Y. Chen et al., 2016). These water resources are essential for ecosystems, agriculture, and water supply for millions of people in Central Asia (Ososkova et al., 2000). Water resources stem from direct precipitation and runoff, seasonal snowmelt as well as meltwater from glaciers and permafrost (Armstrong et al., 2019; Sorg et al., 2012). The glaciers of the Tianshan mountains host the largest amount of fresh water in Central Asia and have a crucial function on the water cycle in the generally arid region of Central Asia (Aizen et al., 1997). Therefore, meltwater from Tianshan is a vital resource for the more than 100 million people living in the arid and semi-arid regions of Central Asia (Lemenkova, 2013; Bekturganov et al., 2016; Xenarios et al., 2019). However, driven by global warming Cen-

44 tral Asia has warmed significantly in recent decades, with a rate of  $0.36\text{--}0.42^\circ\text{C}/10\text{a}$  during  
45 1979–2011 (Z. Hu et al., 2014), resulting in a pronounced glacier retreat and decrease in  
46 snow accumulation in Tianshan Mountains (Aizen et al., 2006; Farinotti et al., 2015). About  
47 97.52% of the glaciers in the Tianshan Mountains show retreating trends from the 1960s  
48 to 2010s (Y. Chen et al., 2016) which is in accordance with the increasing temperature  
49 trend over decades (R. Hu, 2004; Yuan-An et al., 2013). On the contrary, precipitation in  
50 the Tianshan has shown an overall upward trend (Sorg et al., 2012; S. Wang et al., 2013;  
51 Y. Chen et al., 2016; Guan et al., 2021b; Yang & He, 2003; H. Zhang et al., 2009; Yuan  
52 et al., 2004; Fan et al., 2022), although some studies suggest that a significant decrease  
53 in precipitation has been observed in Western Tianshan (Guan et al., 2021b; Z. Hu et al.,  
54 2017). In addition to interannual variability, there is also multi-scale decadal variability in  
55 Tianshan precipitation (Guan et al., 2021b). By using the ensemble empirical mode decom-  
56 position (EEMD) method, Guan et al. (2021a) found that Tianshan winter precipitation  
57 has a multi-decadal oscillation of 26.8 and 44.7 years, and a positive anomaly after 1988.  
58 While summer precipitation has a significant 33.5 years multi-decadal pattern combined  
59 with a nonlinear increasing trend. Both, large-scale atmospheric circulation and individual  
60 weather patterns are key components controlling precipitation and its temporal variability  
61 in the Tianshan Mountains.

62 The Eulerian approach is a common method in studies of regional water vapor trans-  
63 port (Gimeno et al., 2012; Xingang et al., 2007). Previous diagnostics using the Eulerian  
64 method have revealed that the mid-latitude westerlies control the water vapour transport  
65 towards Tianshan. The location and intensity of the westerly jet varies seasonally and is  
66 subject to predominant synoptic patterns (Schiemann et al., 2008; Bothe et al., 2012; Yata-  
67 gai et al., 2012; Yang & He, 2003). It influences the advection of moisture towards the  
68 Tianshan mountains and thus controls the moisture transport from the Atlantic Ocean, the  
69 Mediterranean, and the high latitudes (Aizen et al., 1997; Xingang et al., 2007; Huang et  
70 al., 2013). For instance, the westerly jet axis expands southward in winter and water vapor  
71 is advected mainly from the southwest towards Tianshan (Bothe et al., 2012). Additionally,  
72 there is moisture entering the southwestern Tianshan from Iran and Afghanistan, which is  
73 associated with the intrusion of warm and moist tropical air masses (Aizen et al., 1997).  
74 Contrary, during summer the westerly wind belt moves northward and there is an increase  
75 in water vapour flux from the north and northwest towards the Tianshan Mountains (Bothe  
76 et al., 2012; Huang et al., 2015; Guan et al., 2019). Guo et al. (2014) traced the long-range

77 oceanic water vapour sources affecting the Tianshan region, suggesting that the moisture  
78 sources in the Tianshan during the summer mainly originate from the sub-tropical North  
79 Atlantic Ocean, the Bay of Bengal, the Arabian Sea, and the northern Arctic Ocean. The  
80 Asian monsoon also influences the water vapour transported to the Tianshan Mountains.  
81 During warm El Niño–Southern Oscillation (ENSO) events, anomalous southwestern water-  
82 vapor fluxes from the Arabian Sea and tropical Africa enter Western Tianshan (Mariotti,  
83 2007). In addition to the Eulerian perspective, the isotopic signature of stable water iso-  
84 topes is often used to analyse the leading atmospheric mode of variability and changes.  
85 Results from such studies confirm that precipitation is controlled by the location of the  
86 westerly wind belt and the Indian monsoon (Feng et al., 2013). Simultaneously, the East  
87 Asian monsoon may influence precipitation in the westerly and monsoon transition zones  
88 (J. Yao et al., 2021). S. Wang et al. (2017), however, pointed out that moisture in the  
89 Tianshan Mountains is more likely to be locally sourced. (Song et al., 2019) stated that  
90 the moisture in Urumqi Glacier No.1 mainly comes from Europe and Central Asia, while  
91 the local contribution ranges from 46.8% to 52.1%. It should be mentioned that the Eu-  
92 lerian approach is able to show moisture pathways and moisture transport intensity, but  
93 fails to present a quantitative contribution of individual moisture sources to precipitation  
94 (Gimeno et al., 2012). Besides, the stable water isotope measurements and analyses also  
95 have their limitations and ambiguities due to the complex sensitivity of isotope signals to  
96 various drivers, and issues related to the mixing of isotopic signatures from various sources  
97 into few overall quantities. (Gimeno et al., 2012).

98 The Lagrangian methods have gained popularity in diagnosing moisture transport,  
99 especially in determining the origin of moisture deposited in specific areas (Stohl & James,  
100 2004; Gimeno et al., 2010; Nieto et al., 2006; Durán-Quesada et al., 2010). The main  
101 advantage of the Lagrangian approach is the ability to provide more precise details about  
102 the moisture variation of the air parcels during transport (Gimeno et al., 2012). It allows  
103 simulating the backward trajectory of the air parcel in order to quantitatively describe the  
104 transport process and to identify the source of moisture (Stohl & James, 2004; Sodemann et  
105 al., 2008). Additionally, the Lagrangian analysis is particularly suitable for climatological  
106 studies over decades due to its lower computational cost compared to the more complex  
107 Eulerian moisture tagging approach (Winschall et al., 2014). Numerous attempts have been  
108 performed to determine the moisture sources by using Lagrangian methods (Knippertz &  
109 Wernli, 2010; Ramos et al., 2016; Sun & Wang, 2014; Langhamer et al., 2021). Concerning

110 moisture sources of precipitation in Xinjiang Province of China, S. Yao et al. (2021) used  
111 the Lagrangian diagnostic model FLEXPART to examine the moisture sources contribution  
112 to summer precipitation, concluding that local and Central Asian contributions amount  
113 to over 80%. Similarly, Hua et al. (2017) identified the moisture contribution by using a  
114 dynamical recycling model (DRM) modified by the Lagrangian method, suggesting that the  
115 moisture contribution of summer precipitation in northern Xinjiang during 1982-2010 was  
116 limited from the ocean. The major part of the moisture seems to be derived from land  
117 evaporation in Central Asia, western Siberia, eastern Europe, and northeastern Europe.  
118 Huang et al. (2017) tracked the backward trajectories of extreme precipitation in northern  
119 Xinjiang by the Lagrangian trajectory model HYSPLIT. They state that additionally to  
120 trajectories for rainstorms of above  $100 \text{ mm d}^{-1}$  originating from the North Atlantic, the  
121 Arctic Ocean, and Eurasia, there is also an anomalous branch from the Indian Ocean, which  
122 is closely associated with stronger meridional circulation and especially important for intense  
123 precipitation (Huang et al., 2017). W. Wang et al. (2020), also used the HYSPLIT model  
124 but traced the air particles rather than the actual moisture. They point out that in winter,  
125 western Eurasia contributes the most moisture to the precipitation in northern Xinjiang,  
126 reaching 48.11%. According to these authors, the amount of water vapor contributed by  
127 western Eurasia and the Arctic Ocean to northern Xinjiang shows an increasing trend from  
128 1981-2017 (W. Wang et al., 2020).

129 Although there are many studies using the Lagrangian approach for some Central Asian  
130 sub-regions, especially the Xinjiang province in China, detailed quantitative calculations and  
131 temporal analysis of moisture fluxes to the Tianshan Mountains themselves are still missing.  
132 Besides, some studies taking the Lagrangian perspective have either not considered track-  
133 ing actual moisture (Huang et al., 2017) or have not taken into account changes in specific  
134 humidity along the route (W. Wang et al., 2020). Further, seasonal precipitation varies  
135 greatly in the Tianshan sub-regions: precipitation in the Western Tianshan is concentrated  
136 in spring and winter while the Northern Tianshan receives the most precipitation in spring  
137 and the least in winter. Both the Central and Eastern Tianshan receive the highest pre-  
138 cipitation in summer (Aizen et al., 1997; Guan et al., 2021b). Accordingly, we hypothesize  
139 that the Tianshan sub-regions are served by somewhat different moisture sources in different  
140 seasons, in addition to moisture from the west or Central Asia with the highest flux along  
141 the mid-latitude westerly wind belt.

142 Based on the lack of research in this respect and the advantages of the Lagrangian  
143 approach, we analyse the main moisture sources of the Tianshan Mountains. The temporal  
144 variability and quantitative contribution of moisture sources and favored moisture transport  
145 trajectories are investigated in detail using a verified Lagrangian moisture detection tech-  
146 nique (Sodemann et al., 2008). We focus on four Tianshan sub-regions divisions, namely (1)  
147 Western Tianshan, west of Lake Issyk-Kul, (2) Northern Tianshan, north of Lake Issyk-Kul,  
148 (3) Central Tianshan, south of Ili Valley, (4) Eastern Tianshan, east of the cities of Urumqi  
149 and Dabancheng in China, following the approach taken in (Guan et al., 2021b, 2021a). For  
150 a more detailed description see section 2.1. We then use the Lagrangian analysis tool to  
151 present (a) spatial and temporal moisture flux patterns to the Tianshan Mountains, and (b)  
152 the differences in the main moisture sources between seasons in the four Tianshan Moun-  
153 tains sub-regions. Therefore, the manuscript is arranged as follows: The study area, the  
154 model, and all methods are introduced in Section 2. The model assessment is documented  
155 in Section 3.1. The moisture source patterns and quantitative contributions from individ-  
156 ual moisture source regions to precipitation are presented in Section 3.2 and Section 3.3.  
157 Discussion and conclusion are presented in Sections 4 and 5.

## 158 **2 Study area, data and methods**

### 159 **2.1 Study area**

160 Tianshan Mountains, are a large mountain system in Central Asia, extending 2500 km  
161 from 66°E to 95°E, with an average width of 400 km which mainly straddles the border be-  
162 tween China and Kyrgyzstan (Figure 1). The average elevation of the Tianshan Mountains  
163 is about 5 km, with the highest peak being Tomur Peak at 7,439 meters (42.03 °N, 80.13  
164 °E). Bounded by Issyk-Kul Lake, the eastern edge of Kirgizskiy Alatau and the Fergana  
165 range (boundary 1), the area west of Issyk-Kul Lake is Western Tianshan. The prevailing  
166 air masses are carried into the Tianshan Mountains by moisture-filled westerly winds, and  
167 most of the precipitation falls on the windward western slopes, which results in the overall  
168 heaviest precipitation in the Western Tianshan. The Western Tianshan is under the com-  
169 bined influence of the southwestern branch of the Siberian anticyclone (although to a lesser  
170 extent) and southwestern cyclonic activity during the cold season, resulting in precipitation  
171 occurring mainly in winter and spring. In summer, the influence of subtropical high pres-  
172 sure leads to the least precipitation in the Western Tianshan during that season. Northern  
173 Tianshan lies to the north of Issyk-Kul Lake. In contrast to the Western Tianshan, which

174 receives the most precipitation in winter, the Northern Tianshan is strongly influenced by  
175 the Siberian anticyclonic circulation, resulting in the least amount of winter precipitation.  
176 The most precipitation occurs in spring, related to the development of frontal cyclonic cir-  
177 culation and the influx of cold and wet air masses. Central Tianshan is located in the south  
178 of Ili Valley and is bounded by the Fergana range to the west and by the Kokshaal Too and  
179 Meridionalniy ranges to the south and east. Being surrounded by high mountains prevents  
180 the entry of moisture, resulting in very little winter precipitation in the Central Tianshan,  
181 which only accounts for less than 10 % of the annual precipitation (Aizen et al., 1995; Guan  
182 et al., 2021b). Convection development and unstable atmospheric stratification together  
183 with humid and cold air from the west bring about the maximum precipitation during sum-  
184 mer. Border 3 is bounded by the city of Urumqi and Dabancheng in China. To the east,  
185 the Eastern Tianshan (Region IV) includes the Bogda and Balkan mountain ranges. The  
186 seasonal distribution of Eastern Tianshan precipitation is the same as in Central Tianshan,  
187 with the most precipitation occurring in summer. However, as the area is the least affected  
188 by the East Asian monsoon and westerly circulation, the Eastern Tianshan receives much  
189 less precipitation than the rest of the Tianshan Mountains, averaging only 13 mm in winter  
190 (Guan et al., 2021b).

## 191 **2.2 Data**

192 The basis of the study comprises reanalysis data from the numerical weather prediction  
193 model ERA-Interim provided by the European Centre for Medium-Range Weather Forecasts  
194 (ECMWF) (Berrisford et al., 2011; Dee et al., 2011; Owens & Hewson, 2018) from 1979 to  
195 2017. The usage of reanalysis data is beneficial specifically in remote mountainous regions  
196 with scarce observations (Gerlitz et al., 2014; Zhao et al., 2020). The reliability of ERA-  
197 Interim in Central Asia has been verified by long-term trend analysis (Z. Hu et al., 2016;  
198 Hamm et al., 2020; Liu & Zhang, 2017; S. Chen et al., 2019). We use the global ERA-Interim  
199 reanalysis dataset with its horizontal resolution of  $0.75^\circ \times 0.75^\circ$  and 60 vertical levels, from  
200 the surface to 0.1 hPa. In particular, the 3-D wind field, the specific humidity, the surface  
201 pressure, the Planetary Boundary Layer (PBL) height, and the 2-m air temperature serve  
202 as input variables to perform a moisture source detection study. The PBL height is scaled  
203 by the factor of 1.5 to counteract the underestimation of the PBL height specifically over  
204 maritime and mountainous terrain (Sodemann et al., 2008; Weigel et al., 2007; Zeng et  
205 al., 2004). The conversion into pressure coordinates considers a constant lapse rate of

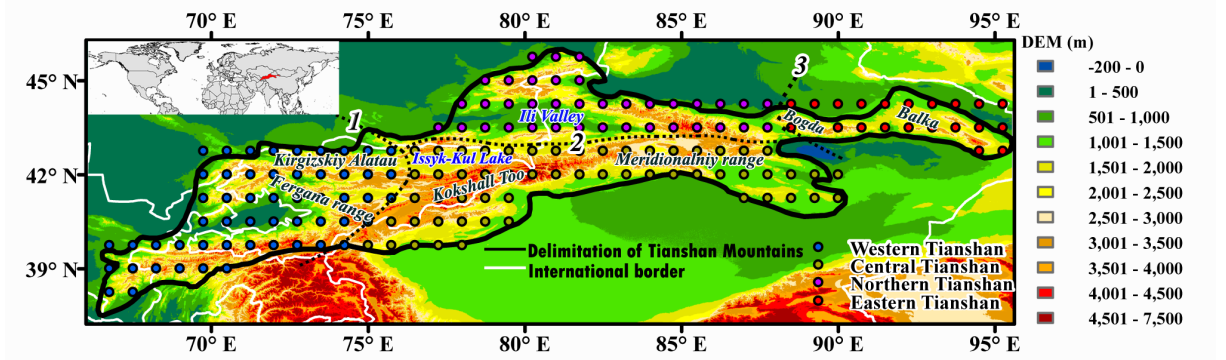


**Figure 1.** Topography of the study area and the starting points of backward trajectories within the Tianshan mountains. The dotted lines numbered 1 to 3 refer to the borders between the four sub-regions of the Tianshan Mountains detailed in the text. The red area in the small map in the upper left corner shows the position of the Tianshan Mountains in the Northern Hemisphere. Four differently colored sets of dots represent the initial positions over the Western Tianshan (blue dots), Northern Tianshan (purple dots), Central Tianshan (yellow dots), and Eastern Tianshan (red dots).

206  $\gamma = 0.0065 \text{ K m}^{-1}$  (Langhamer et al., 2018). Additionally, we use the ERA-Interim monthly  
 207 precipitation data, and the precipitation product from the Global Precipitation Climatology  
 208 Centre (GPCC) (Schneider et al., 2018) to validate the performance of the Lagrangian  
 209 model.

### 210 **2.3 Lagrangian method for determining evaporative moisture sources**

211 The Lagrangian perspective transforms the spatially stationary point of view from  
 212 gridded reanalysis data into that of traveling air parcels. Along trajectories, changes in  
 213 physical quantities such as moisture, air pressure, and temperature can be analyzed. We  
 214 apply the Lagrangian analysis tool Version 2.0 (LAGRANTO) (Sprenger & Wernli, 2015),  
 215 version 1.0 by (Wernli & Davies, 1997) to calculate trajectories 15 days backward in time.  
 216 The backward trajectories start from a  $0.75^\circ$  regular grid within four predefined sub-regions  
 217 encompassing the Tianshan Mountains. The grid is vertically subdivided in 11 equally  
 218 spaced ( $\Delta p = 50 \text{ h Pa}$ ) levels from the surface to 500 h Pa above ground level which encloses  
 219 the majority of the precipitable water of the Tianshan Mountains. This set-up comprises  
 220 242, 407, 594, and 616 grid points in Eastern, Northern, Western and Central Tianshan  
 221 (Figure 1). Every reanalysis time step of 6 hours contains 242, 407, 594, and 616 15-d

222 backward trajectories, respectively. This results in over 200 million trajectories to represent  
 223 a 37-year climatology of moisture sources of the Tianshan Mountains. Thereby the moisture  
 224 source detection method developed by Sodemann et al. (2008) was applied, which is based  
 225 on the moisture tracing the concept of Stohl and James (2004). This method includes the  
 226 conservation of specific humidity  $q$  within the air parcel of mass  $m$  where the increase in  
 227 specific humidity within a calculation time step  $i$  of the trajectory results only from moisture  
 228 uptake through evaporation  $E$ , while the decrease occurs due to precipitation  $P$ ,

$$m \frac{dq_i}{dt} = E_i - P_i \quad . \quad (1)$$

229 Multiple moisture uptakes can occur along a 15-day backward trajectory. Therefore, all new  
 230 moisture uptakes  $dq_j$  are weighted with respect to the amount of pre-existing moisture  $q_i$   
 231 resulting in a fractional contribution  $f_j$  of each moisture uptake location,

$$f_j = \frac{dq_j}{q_i} \quad . \quad (2)$$

232 Precipitation along the trajectory reduces the impact of the previously estimated moisture  
 233 uptake and is partially subtracted according to their fractional contribution (Sodemann et  
 234 al., 2008). The conversion of the specific humidity decrease  $\Delta q_{k,t=0}$  above the study region  
 235 into the 6 hourly precipitation sum can be expressed as,

$$P = -\frac{1}{g} \sum_k \Delta q_{k,t=0h} \cdot 10^{-3} \cdot \Delta p_k, \quad (3)$$

236 where  $g$  is the the gravitational acceleration,  $k$  is the vertical index of the 11 equidistant  
 237 ( $\Delta p_k = 4990$  h Pa) levels and is hereinafter called Lagrangian precipitation (Sodemann et  
 238 al., 2008). Based on the Lagrangian precipitation and the fractional contribution of each  
 239 moisture uptake along the trajectory, the amount of evaporation is calculated and assigned  
 240 to the surface according to,

$$E_j = P_{i=0h} \cdot f_m \quad . \quad (4)$$

241 Following the concept of Sodemann et al. (2008), only trajectories that cause precipi-  
 242 tation are selected in the calculation. The selection criterion for trajectories was that the  
 243 relative humidity exceeded 80% and the specific humidity decreases. Originally, Sodemann  
 244 et al. (2008) considered only a moisture increase within the PBL as evaporative moisture  
 245 source. Subsequently, Sodemann and Zubler (2010) deviate moisture sources within and  
 246 above PBL moisture uptake. The authors concluded to consider moisture increase in the  
 247 free atmosphere as evaporative moisture source only if the spatial and temporal pattern of

248 the combined above and below PBL moisture uptake shows similarities to the within PBL  
249 moisture uptake.

250 In addition, this study investigates linear trends of defined moisture sources in winter  
251 and summer using the Mann-Kendall (M-K) test (Mann, 1945; Kendall, 1975). We also use  
252 Mann-Kendall (M-K) correlation coefficient (Freedman et al., 2007) to assess the statistical  
253 significance of any correlation analysis.

### 254 **3 Results**

#### 255 **3.1 Characteristics of ERA-Interim precipitation, GPCC precipitation and La-** 256 **grangian precipitation estimates**

257 At first, we validate the Lagrangian precipitation estimates (Equation 3) over the Tian-  
258 shan Mountains against the 6-hourly forecasts from ERA-Interim and the GPCC precip-  
259 itation. The spatial distributions of ERA-Interim precipitation over Tianshan Mountains  
260 are shown in Figures 2(e)-2(h). Precipitation over the Tianshan Mountains has a strong  
261 seasonality with the larger precipitation amounts in MAM and JJA. Regionally, the west-  
262 ern part of Tianshan receives the most precipitation and Eastern Tianshan has relatively  
263 less precipitation throughout the year. These spatial and seasonal distributions are further  
264 confirmed by the GPCC precipitation (Figures 2(i)-2(l)). However, the precipitation from  
265 ERA-Interim is obviously higher than that from the GPCC. Previous studies have found  
266 that mountainous and complex topographic areas result in large differences in precipitation  
267 between products (Hamm et al., 2020). Gao et al. (2018) reported ERA-Interim overestima-  
268 tion of daily mean and extreme precipitation on the Tibetan Plateau. Similar conclusions  
269 were drawn by Hamm et al. (2020), founding that total spatially averaged precipitation for  
270 the period May to September 2017 from ERA-Interim (781 mm) over the Central Himalaya  
271 and the Southwest Tibetan Plateau, was much higher than that from GPCC precipitation  
272 (411 mm).

273 Figures 2(a)-2(d) display the composite mean horizontal distribution of estimated pre-  
274 cipitation based on the Lagrangian approach (Equation 3) over the Tianshan Mountains.  
275 The Lagrangian estimated precipitation reasonably captured the major spatial patterns and  
276 seasonality of precipitation in the Tianshan Mountains similar to ERA-Interim (Figures 2(e)-  
277 2(h)). The Lagrangian precipitation estimates are somewhat higher than the ERA-interim

278 precipitation when considering individual grid points. This is especially observed in the  
 279 Western and Northern Tianshan.

280 Figure 3(a) visualizes the comparison of monthly precipitation between the three pre-  
 281 cipitation data sets. The Lagrangian precipitation and ERA-Interim precipitation as well  
 282 as the Lagrangian precipitation and GPCC precipitation both show statistically significant  
 283 correlations ( $p \leq 0.05$ ) with  $R^2=0.98$  and  $R^2=0.95$ , respectively. Nevertheless, the ERA-  
 284 Interim precipitation does not fully reflect some of the details of the GPCC data. The peak  
 285 of monthly precipitation occurs in May (Lagrangian precipitation and GPCC precipitation),  
 286 while ERA-Interim displays a single peak with the highest value in June. Similarly, pre-  
 287 cipitation in October is higher than in September, a feature that is not picked up in the  
 288 ERA-Interim data. In addition, Figure 3(b) demonstrates that the Lagrangian approach  
 289 is quite efficient in the Tianshan Mountains. A statistically significant linear relationship  
 290 ( $R^2 = 0.99$ ) is shown between monthly evaporation (the sum of evaporation above and  
 291 within the boundary layer) and Lagrangian precipitation estimates. Therefore, following  
 292 e.g. Langhamer et al. (2021); Schuster et al. (2021), it is plausible that we apply the  
 293 Lagrangian method to detect moisture sources of the Tianshan Mountains.

### 294 **3.2 Patterns of moisture sources of Tianshan precipitation**

295 Figure 4(a), (b), and (c) show the diagnostic picture of all attributed moisture sources,  
 296 the attributed evaporation inside the PBL and from above the PBL, respectively. Moisture  
 297 sources within the PBL show a similar spatial pattern to that of all attributed moisture  
 298 sources, with the highest evaporative moisture contribution area mainly concentrated in  
 299 the Tianshan itself. Regions with moisture source contributions exceeding 0.2 mm/month  
 300 concentrate in Western Tianshan. Moisture source contributions exceed 0.1 mm/month  
 301 over the majority of Tianshan, indicating that local evapotranspiration (i.e., recycling of  
 302 continental moisture) are the major moisture source in the Tianshan Mountain. In addition,  
 303 much of the moisture was also tracked back to West Asia, and even the Arabian Gulf. It  
 304 is worth noting that the location of the annual mean source of moisture uptake above the  
 305 PBL (Figure 4c) is quite similar to the location within the PBL (Figure 4b). Although,  
 306 according to the Lagrangian approach, the location of the moisture source can only be  
 307 determined when an increase in specific humidity below the top of the PBL is measured  
 308 (Sodemann et al., 2008). However, Sodemann and Zubler (2010) pointed out that if the  
 309 patterns of moisture sources above and within the PBL are similar, it is hardly possible

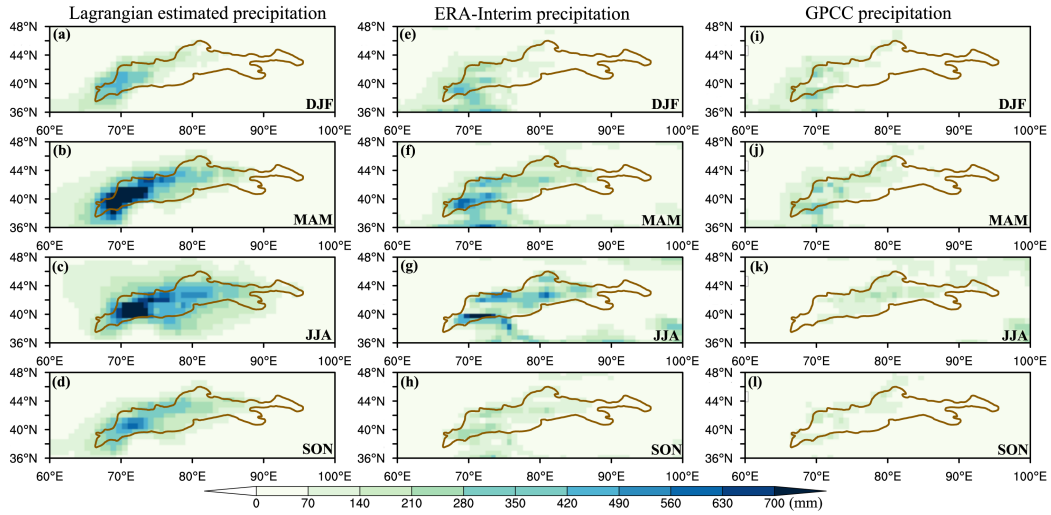


**Figure 2.** Spatial distribution of seasonal precipitation in Tianshan Mountains (mm) from the ERA-Interim Lagrangian estimated precipitation (left), the ERA-Interim monthly precipitation (middle), and the GPCC precipitation (right) during 1979 - 2017. All datasets are averaged in the four seasons: March-May (MAM), June-August (JJA), September-November (SON), and December-February (DJF). The area of the Tianshan Mountains is delineated with an earthy yellow polygon.

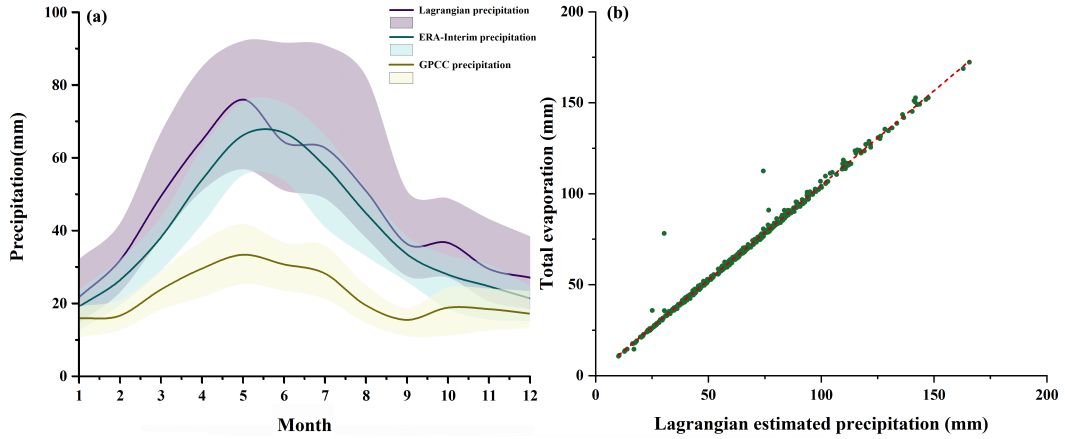


**Figure 3.** (a) ERA-Interim estimated monthly precipitation in the Tianshan Mountains, compared with that derived from the ERA-Interim and GPCC precipitation. The solid lines are the median; the areas filled correspond to the interquartile range. (b) The monthly Lagrangian estimated precipitation and the total local evaporation of the Tianshan Mountains.

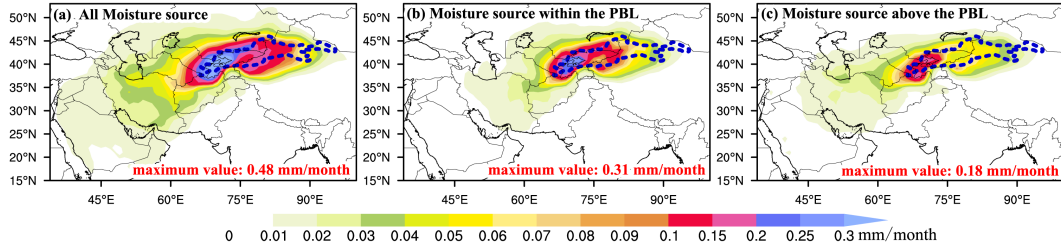


**Figure 4.** Spatial patterns of (a) all average annual attributed evaporative moisture sources (mm/month); (b) average annual attributed evaporative moisture sources within PBL; (c) average annual attributed evaporative moisture sources above the PBL of the Tianshan precipitation for the period from 1979 to 2017. The curve in blue dashed is the border of the Tianshan Mountains.

310 that the moisture sources of precipitation in the study area can be significantly different  
 311 within and above the PBL. Therefore, in the following, we attribute the increase in specific  
 312 humidity above the PBL also to evaporation from the surface, i.e., consider all the attributed  
 313 moisture as the sources of precipitation in the Tianshan Mountains.

314 We subdivide the moisture sources presented into two seasons, thereby, October-March  
 315 denoted as winter, and April-September as summer. South-westerly water vapour flux  
 316 prevails into the Tianshan Mountains in winter (Figure 5e). Low latitudes and the Atlantic  
 317 Ocean regions show relatively high precipitable water vapour (PWC) values compared to  
 318 low PWC values over Central and East Asia including the Tianshan Mountains themselves.  
 319 From the Euler perspective, there are two main water vapour pathways into the Tianshan  
 320 Mountains in winter. One of them is a long-range water vapor transport pathway, advected  
 321 predominantly by westerlies, extending from the Atlantic Ocean, the European continent,  
 322 the Mediterranean Sea, and the Caspian Sea to the Tianshan. The second most important  
 323 moisture pathway towards Western Tianshan stems from the Indian Ocean and the Arabian  
 324 Peninsula (Figure 5e). From the Lagrangian perspective (Figure 5a-d), the moisture sources  
 325 of Tianshan extend as far west as 30°W over the Atlantic Ocean based on a minimal lower  
 326 threshold of 0.0002 mm/month. Areas with larger moisture uptake are mainly located  
 327 over Central and West Asia, with the highest values centered in and around the Western  
 328 Tianshan. Although the moisture-source regions in winter of the different sub-regions of  
 329 Tianshan Mountains look relatively similar, the source area for the Western Tianshan is  
 330 markedly expanded both to the west and to the southeast (Figure 5a). In contrast, uptake  
 331 locations for the Central Tianshan are confined to areas east of the Prime meridian (Figure

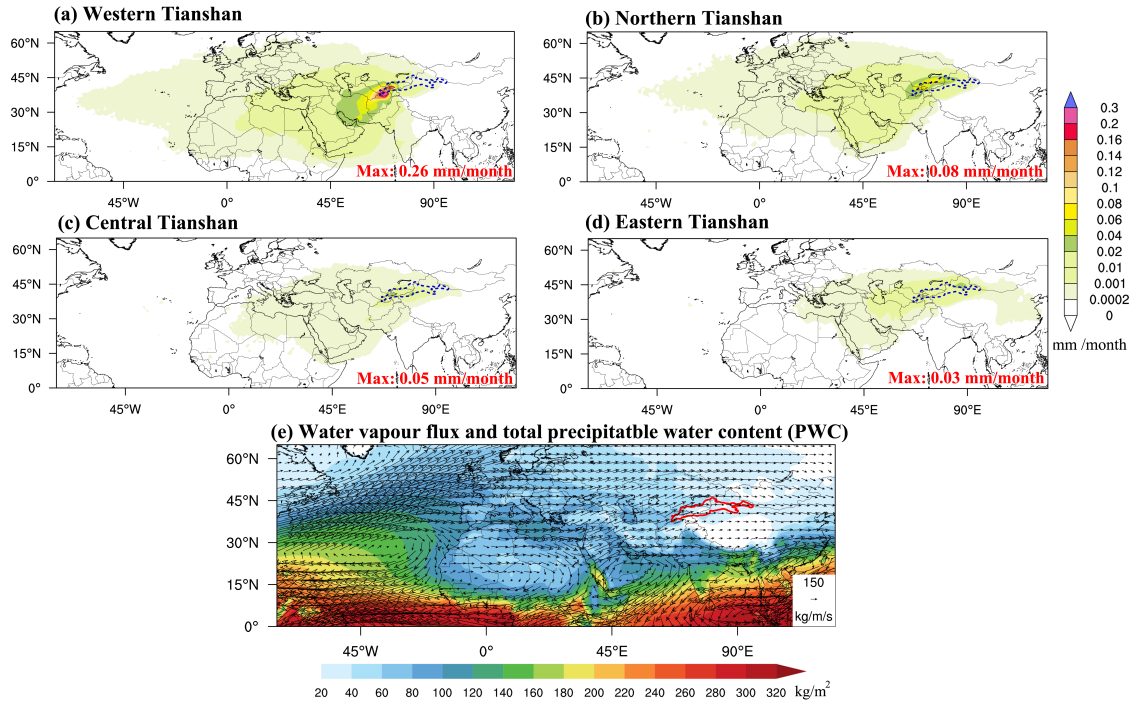


**Figure 5.** Spatial patterns of average attributed evaporative moisture sources (mm/month) of the different sub-regions (a)-(d) of the Tianshan mountains in winter; the polygon in blue dashed is the border of the Tianshan Mountains; (e) Water vapour flux (vector in kg/m/s) and total precipitable water vapour content (PWC in kg/m<sup>2</sup>) in winter. The area of the Tianshan Mountains is delineated with a red polygon in (e).

332 5c). The area of uptake for the Eastern Tianshan is even narrower to roughly east of  
 333 30°E (Figure 5d). Regions with evaporative moisture sources for the Western Tianshan  
 334 exceeding 0.1 mm/month have a widespread distribution that extends southwestward to the  
 335 Iranian Plateau. Areas outside the Tianshan with evaporative moisture sources exceeding  
 336 0.1 mm/month are rare for the other three Tianshan sub-regions. Moisture sources for  
 337 the Western Tianshan in winter extend southeastward to the Indian Peninsula until 80°E  
 338 using a threshold of 0.0002 mm/month, which is not the case for any of the other Tianshan  
 339 sub-regions.

340 PWC values in summer are higher ( $> 125 \text{ kg/m}^2$ ) over the continental regions at  
 341 mid-to-high latitudes compared to winter (Figure 6e). The presence of the Iranian High  
 342 Pressure advects water vapour from high-latitude Eurasia towards the Tianshan Mountains.  
 343 Meanwhile, this anticyclone blocks water vapour entering the Tianshan from the southwest.

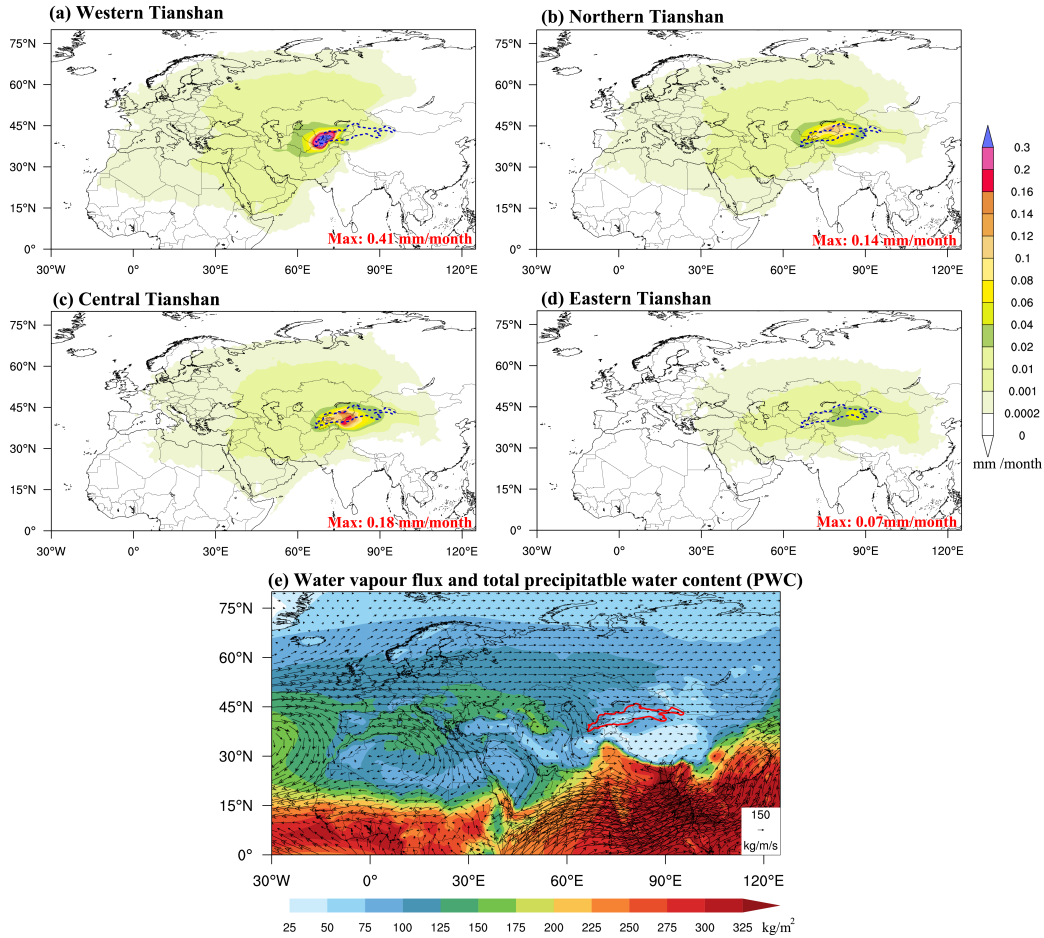


**Figure 6.** Spatial patterns of average attributed evaporative moisture sources (mm/month) of the four sub-regions (a)-(d) of the Tianshan Mountains in winter; the curve in blue dashed is the border of the Tianshan Mountains; (e) Water vapour flux (vector in kg/m/s) and total precipitable water vapour content (PWC in kg/m<sup>2</sup>) in summer. The area of the Tianshan Mountains is delineated with a red polygon in (e).

344 In summer, the area of moisture contribution is generally smaller to the west and to the  
 345 south, confined to areas east of the Prime meridian (Figure 6a-c). The moisture source of  
 346 the Eastern Tianshan is limited to east of 30°E (Figure 6d). The moisture contribution is  
 347 more locally concentrated. The area of moisture uptake in the high latitudes of Eurasia  
 348 expands further to 75° N with an increased contribution from high latitude Eurasia. Simul-  
 349 taneously, the contribution from the Arabian Peninsula and the Iranian Plateau is smaller  
 350 than in the winter. The summer moisture source in the Eastern Tianshan extends even  
 351 further eastward to 120°E in East Asia (Figure 6d).

### 3.3 Quantitative contribution from individual moisture source regions

The previous section showed that sources of water vapor contributing to precipitation in the Tianshan Mountains extend in the West to the Atlantic Ocean and Europe, in the North to Europe, in the Southwest to West Asia and the Indian Ocean, and in the Northeast to East Asia and Siberia. To more precisely describe the key moisture sources of precipitation in Tianshan Mountains, we define 10 separate moisture uptake regions in the Northern Hemisphere (Figure 7) and additionally the Tianshan Mountains themselves (TS) as the source region of local evaporation following an approach similar to (Sodemann et al., 2008) and S. Yao et al. (2021). The terrestrial part includes Central Asia (CA) where the Tianshan Mountains are located, West Asia (WA) and North Africa (NA), and the European region (EU) which lies to the northwest of the Tianshan Mountains. We further separate into the Siberian region (SR) and East and Southeast Asia (ESA) in the east of the Tianshan Mountains. The oceanic part includes the North Atlantic Ocean (NO), the Mediterranean Sea (MS), the Caspian Sea (CS), and the Indian Ocean (IO). Some inland seas, such as the Baltic Sea and the Black Sea, are incorporated into the European region owing to their low contribution and their location within Europe. The contribution of a particular region is evaluated as the ratio of the integral of its moisture contributing area to the integral of all identified moisture contributing areas. The 11 areas shown in Figure 9 contribute more than 99.5% of all moisture flux to the precipitation in the Tianshan Mountains. Hence, all key moisture source areas of precipitation over the Tianshan Mountains are included in this assessment.

Central Asia is the dominant source of moisture for all sub-Tianshan. For the Western Tianshan, the contribution of Central Asia shows a single-peak pattern (Figure 8a). From April to October, Central Asia is the major contributor of moisture in the Western Tianshan, with a contribution of on average 41.4%, and 46.3% in August (Figure 8a). In contrast, from November to March, West Asia replaces Central Asia as the largest source of moisture in providing precipitation for the Western Tianshan, accounting for almost 50% of the total. The third source of moisture stems from the Tianshan itself (local evaporation) with 17.2%, also showing a single-peak pattern in summer. Moisture from the Indian Ocean also contributes considerably (7.2%) to precipitation in the Western Tianshan in winter, while Europe contributes 9.5% of the precipitation in summer (Figure 8a). For Northern Tianshan, the continent is the most vital moisture source for precipitation (Figure 8b). The four moisture source regions with mean relative contributions  $\geq 5\%$  include local evaporation

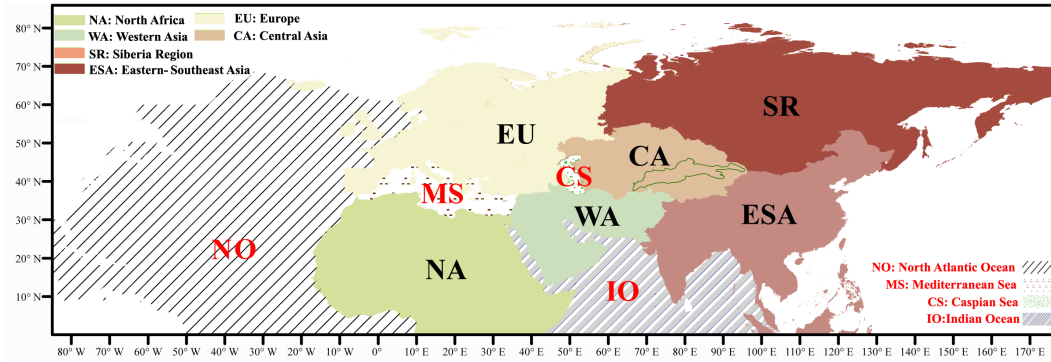


**Figure 7.** Definition of the ten regions for diagnosing and attributing moisture sources in this study: Central Asia (CA), West Asia (WA), North Africa (NA), Europe (EU), Siberia (SR), East and Southeast Asia (ESA), North Atlantic Ocean (NO), Mediterranean Sea (MS), Caspian Sea (CS), and Indian Ocean (IO). The area of the Tianshan Mountains (TS) defining the area of local evaporation is delineated with a green polygon.

385 (22.5%), Central Asia (37.0%), West Asia (19.5%), and Europe (7.3%). It is noteworthy  
 386 that the local moisture contribution accounted for 46.6% in August, providing the largest  
 387 source of moisture in the Northern Tianshan. The moisture contribution to the Central  
 388 Tianshan is very similar to the monthly distribution of the Western Tianshan, although  
 389 local evaporation provides a very uniform share throughout the year of about one-third.  
 390 The relative contribution of moisture from Central Asia to the Central Tianshan is larger  
 391 than to the Western Tianshan and also more evenly distributed across seasons (Figure 8c).  
 392 In addition to the largest contribution coming from Central Asia and local evaporation  
 393 (66.8%), West Asia adds another 18.0%. Hence, these three regions contribute up to almost  
 394 85% of the moisture to the Central Tianshan. For the Eastern Tianshan, Central Asia is  
 395 the moisture source with an unassailable position of precipitation in all seasons, accounting  
 396 for above 45% (Figure 8d). It is followed by local supply, evenly distributed in all months  
 397 except for March, and overall accounting for 23.4%. The other two moisture sources with  
 398 mean relative contributions of more than 5% are West Asia (10.4%) and Europe (5.3%),  
 399 respectively. The contribution of Europe to summer precipitation in the Eastern Tianshan  
 400 is reduced compared to that in winter. East and Southeast Asia, and the Siberian region,  
 401 replacing Europe, are the other two important moisture sources with a percentage in summer  
 402 of 7.7% and 5.2%, respectively (8d).

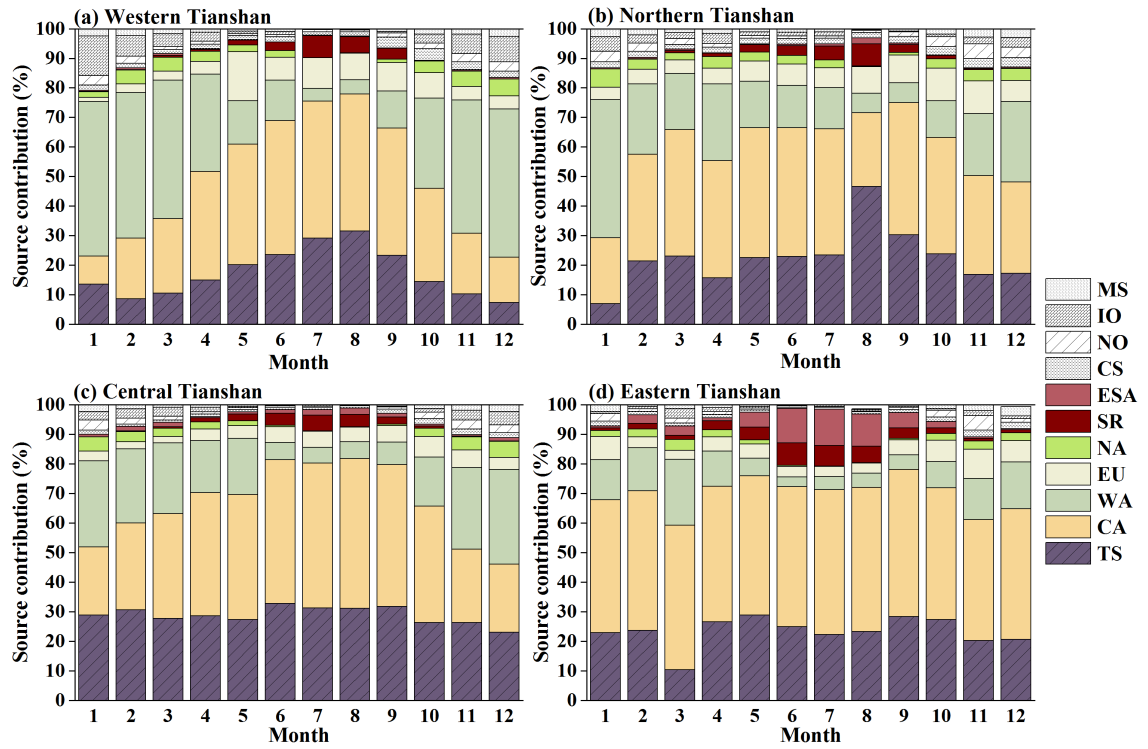


**Figure 8.** Monthly mean relative contribution of the different uptake sectors defined in Figure 7 to the attributable precipitation over the (a) Western Tianshan, (b) Northern Tianshan, (c) Central Tianshan, and (d) Eastern Tianshan.

403 We further investigate the possible correlations between the contribution of each identi-  
404 fied moisture source area and precipitation in the Tianshan Mountains in winter and summer  
405 in the time series of annual values of the study period (Table 1). For the Western Tianshan,  
406 the winter precipitation sum is significantly positively correlated with the moisture contri-  
407 bution from West Asia and the Indian Ocean, and negatively correlated with the moisture  
408 contribution from local sources and Central Asia, strongly confirming that moisture from  
409 the southwest plays a dominant role in the increased winter precipitation in the Western  
410 Tianshan. Winter precipitation in the Western Tianshan is positively correlated with the  
411 moisture contribution from East and South Asia, implying that the source of moisture from  
412 the East to the Western Tianshan, although low, should not be neglected. Precipitation  
413 in the Northern Tianshan is significantly positively correlated with moisture contribution  
414 from the Caspian Sea and the Mediterranean Sea and negatively correlated with local mois-  
415 ture contribution in winter, reflecting the profound influence of the westerlies on winter  
416 precipitation in the Northern Tianshan. The winter precipitation in ERA-Interim shows  
417 no significant correlation with any moisture source in the Central and Eastern Tianshan,  
418 while precipitation in GPCC is positively correlated with moisture from North Africa and  
419 the Indian Ocean for the Central Tianshan and negatively correlated with local moisture  
420 contribution for the Eastern Tianshan (Table 1).

421 In general, there is no obvious trend in the contribution from most source regions in  
422 winter during 1979-2017. However, Tianshan, the region of local sources, and Central Asia  
423 show a significant decreasing trend ( $p \leq 0.05$ ) of moisture contribution to the Eastern Tian-  
424 shan in winter with linear trends of  $-0.30\text{mm}/10\text{a}$  and  $-0.11\text{mm}/10\text{a}$ , respectively (Figure  
425 9). The finding is consistent with a decreasing trend in Winter precipitation in the East-  
426 ern Tianshan in the ERA-Interim data. However, (Guan et al., 2021a) derive a positive  
427 precipitation trend for the Eastern Tianshan in winter based on GPCC data for the same  
428 period.

429 Correlations between summer precipitation from ERA-Interim and GPCC in the Tian-  
430 shan Mountains and the moisture source contribution vary widely. In general, summer  
431 precipitation in the Western Tianshan has a negative correlation with moisture from Eu-  
432 rope and is positively correlated with moisture from East Asia. In addition, precipitation  
433 remains significantly positively correlated with moisture contribution from the southwest.  
434 Different from winter, the summer precipitation in the Northern Tianshan is negatively  
435 correlated with moisture flux from the Caspian Sea and the Atlantic Ocean (Table 1). Not

**Table 1.** Correlation between moisture uptake in the source areas according to Figure 7 and ERA-Interim precipitation based on seasonal values in the period 1979-2017; correlation coefficients with moisture uptake and GPCC precipitation are shown in parentheses. Mann-Kendall (M-K) correlation coefficients were calculated for winter and summer. Only coefficients of statistically significant correlations ( $p \leq 0.05$ ) are presented in the table; WT: Western Tianshan, NT: Northern Tianshan, CT: Central Tianshan, ET: Eastern Tianshan.

	Winter				Summer			
	WT	NT	CT	ET	WT	NT	CT	ET
TS	(-0.26)	-0.27 (-0.33)		(-0.31)	(-0.41)		(-0.43)	
CA	-0.47 (-0.35)							
WA	0.29 (0.29)				(0.28)		(0.24)	
EU					-0.21		(-0.24)	
NA			(0.24)		(0.23)			
SR								0.41
ESA	0.32 (0.28)				0.23		(0.23)	
CS		0.23 (0.24)					-0.33	
NO							-0.22	
IO	0.30 (0.27)		(0.24)		0.24	(0.31)	(0.31)	
MS		0.34 (0.35)					(0.27)	

436 surprisingly, summer precipitation in the Eastern Tianshan is significantly positively cor-  
 437 related with moisture from Siberia. We find significantly decreasing trends of moisture  
 438 contribution from the North Atlantic Ocean for Northern Tianshan (-0.05 mm/10a), Cen-  
 439 tral Tianshan (-0.02 mm/10a) and Eastern Tianshan (-0.01 mm/10a) and from Europe for  
 440 Central Tianshan (-0.06 mm/10a) and Eastern Tianshan (-0.03 mm/10a) over the study  
 441 period (Figure 10). These trends do not play out in decreasing precipitation amounts ac-  
 442 cording to (Guan et al., 2021a), presumably because their relative contribution to the overall  
 443 precipitation in summer in the respective sub-regions of Tianshan is limited.

444 We selected monthly precipitation from ERA-Interim data exceeding the 95th percentile  
 445 in winter and summer in each Tianshan region as extreme precipitation months. Clear  
 446 differences in the spatial pattern of source regions of moisture received by the four sub-

447 Tianshan during extreme precipitation are evident in Figure 11 and Figure 12. Compared  
448 with the average evaporative moisture intake, the overall amount during extreme winter  
449 precipitation in Western Tianshan increased by 28.9%, with the main increase still coming  
450 from the southwest. (Figure 11(a)). The relative moisture contributions from West Asia and  
451 the Indian Ocean for extreme precipitation are 54.3% and 7.9% (Figure 13), with moisture  
452 uptakes increasing from 19.8 mm/month and 2.4 mm/month (average in winter) to 32.7  
453 mm/month and 4.8 mm/month, respectively from these regions. The moisture contribution  
454 from Europe, on the contrary, decreases from 4.2% (winter average share) to 1.6%, a decrease  
455 of 69.2%, implying that extreme precipitation in the Western Tianshan in winter is caused  
456 by enhanced meridional moisture advection and weakened latitudinal moisture flux. For  
457 the Eastern Tianshan, the relative contributions from Siberia as well as from East and  
458 South Asia during winter extreme precipitation increase from 1.3% and 1.7% to 5.6% and  
459 10.1%, respectively (Figure 13 (d)). The moisture uptakes increase from 0.03 mm/month  
460 and 0.01 mm/month to 0.50 mm/month and 0.94 mm/month, respectively (Figure 11 (d)),  
461 reaffirming the importance of moisture from the east for the Eastern Tianshan. Although  
462 Europe accounts for only 7.1% of the moisture contribution in the Northern Tianshan during  
463 winter (Figure 8), the largest increase of 64.8% in moisture contribution from Europe is  
464 observed during extreme winter precipitation, suggesting that moisture from Europe is an  
465 important cause of extreme precipitation in the Northern Tianshan, which is diametrically  
466 opposed to the Western Tianshan. For the Central Tianshan, Central Asian and local  
467 evaporation plays a crucial role during extreme precipitation, especially for Central Asia,  
468 where the relative contribution goes up from 29.1% (average in winter) to 39.3% (Figure  
469 13). The increase in moisture uptake is close to 50% in both cases. However, it can  
470 be seen from the (Figure 11 (c)) that the regions of increased moisture contribution are  
471 concentrated in and around the Central Tianshan itself, demonstrating that the extreme  
472 winter precipitation moisture contribution in the Central Tianshan is derived from local  
473 evaporation. In contrast to winter, the increased moisture contribution during extreme  
474 summer precipitation is concentrated locally and in Central Asia, especially for the Central  
475 and Northern Tianshan (Figure 12. Not surprisingly, the contribution of moisture from  
476 Siberia as well as East and South Asia appears to increase during extreme precipitation in  
477 the Eastern Tianshan, with the relative moisture contributions from these regions increasing  
478 from 5.2% and 7.7% (summer average shares) to 9.9% and 18.5%, respectively (Figure 13).

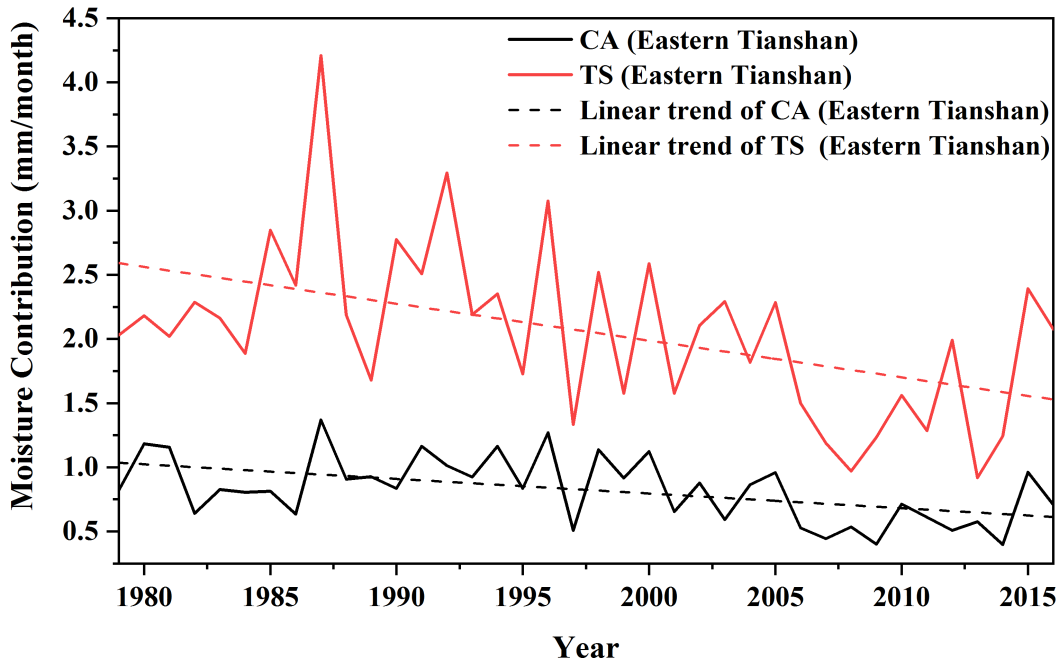


**Figure 9.** Time series of moisture contribution from Central Asia and local sources for the Eastern Tianshan in winter during the 1979-2017.

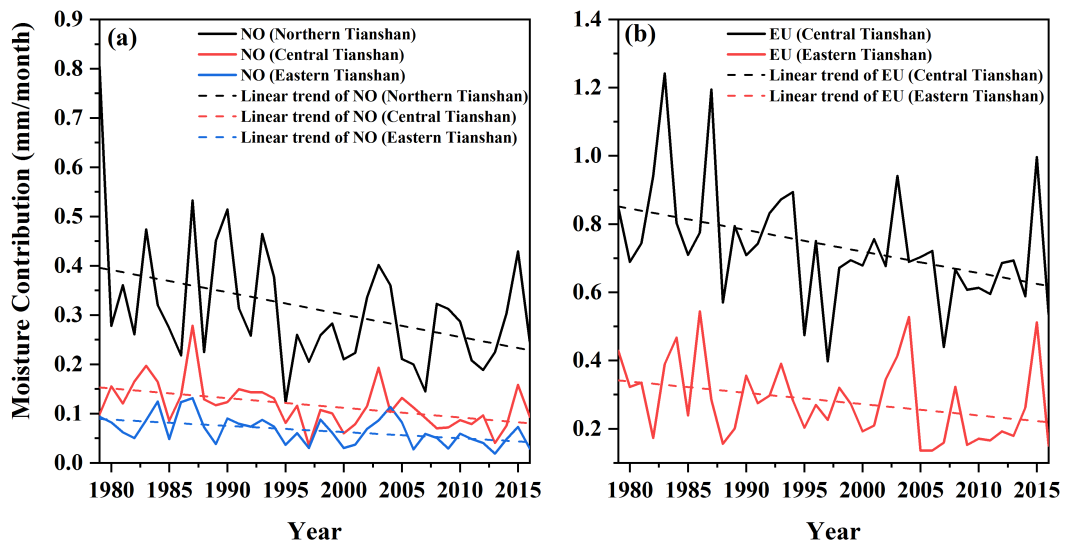


**Figure 10.** Time series of moisture contribution in summer from the North Atlantic Ocean for Northern, Central and Eastern Tianshan, respectively (a) and Europe (b) for Central Tianshan and Eastern Tianshan during 1979-2017.

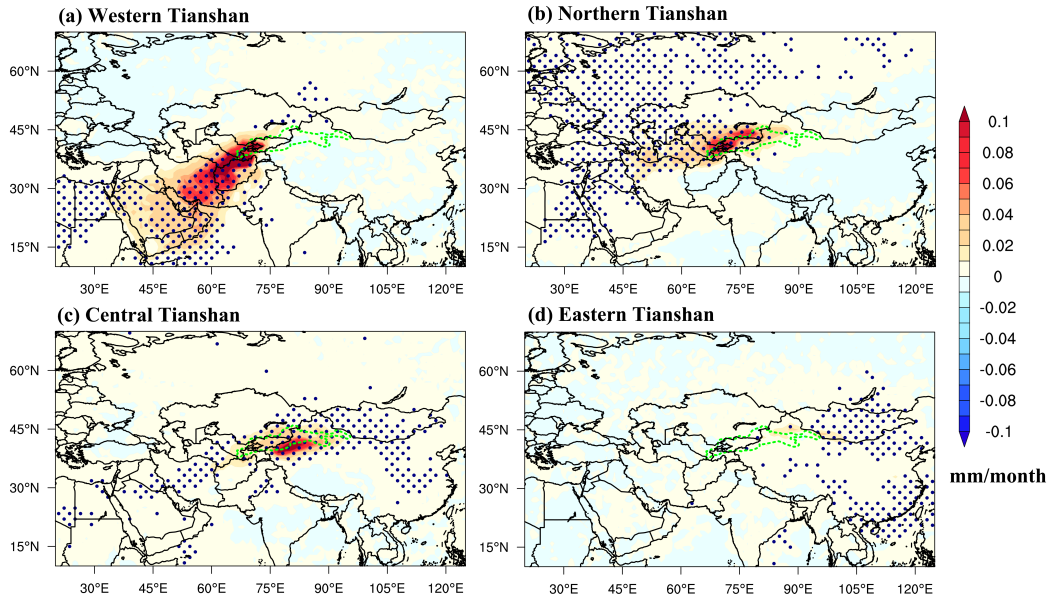


**Figure 11.** Anomalies of evaporative moisture sources during extreme winter precipitation in (a) Western Tianshan, (b) Northern Tianshan, (c) Central Tianshan, and (d) Eastern Tianshan. The area of the Tianshan Mountains is delineated with a green polygon and the blue dotted areas indicate anomalies that are significant at the 95% confidence level.

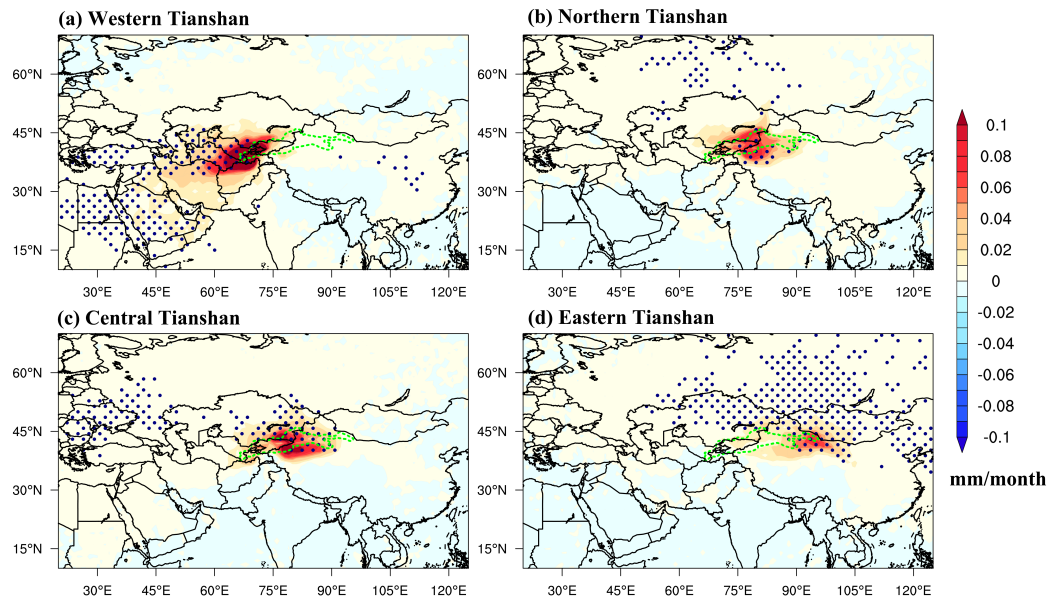


**Figure 12.** Anomalies of evaporative moisture sources during extreme summer precipitation in (a) Western Tianshan, (b) Northern Tianshan, (c) Central Tianshan, and (d) Eastern Tianshan. The area of the Tianshan Mountains is delineated with a green polygon and the blue dotted areas indicate where anomalies are significant at the 95% confidence level.

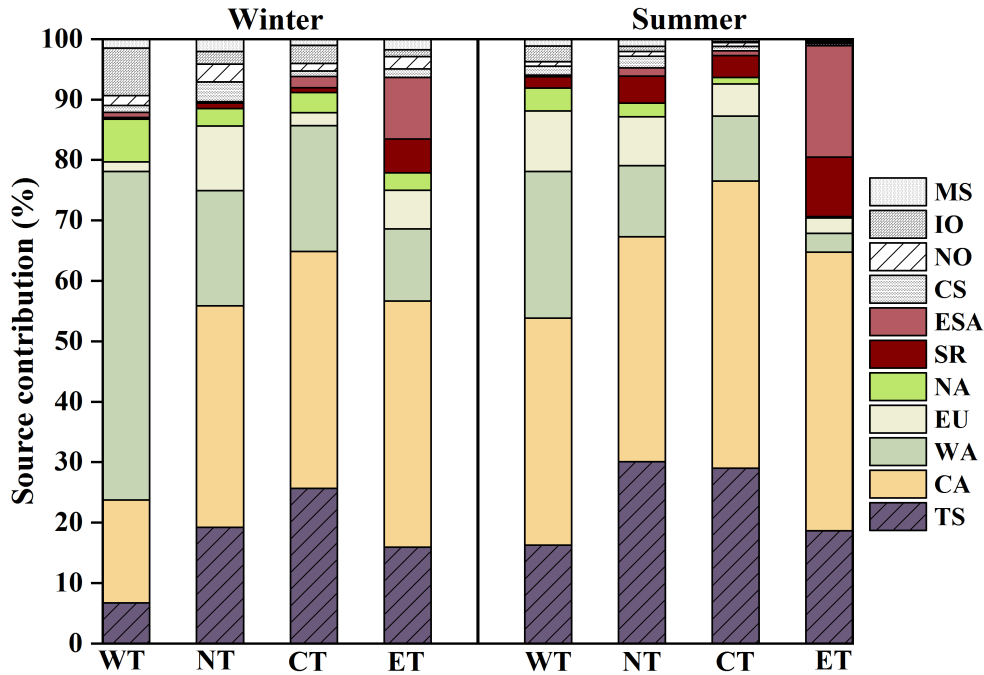


**Figure 13.** Monthly mean relative contribution of the different uptake sectors defined in Figure 7 to the attributable precipitation over the Western Tianshan (WT), Northern Tianshan (NT), Central Tianshan (CT), and Eastern Tianshan (ET) in winter and summer.

#### 4 Discussion

According to Guan et al. (2021b), most parts of Tianshan experienced increasing precipitation during 1950-2016, especially in the Northern, Central, and Eastern Tianshan. They suggested possible reasons for the variability of precipitation in terms of atmospheric circulation. The East Atlantic-West Russia (EATL/WRUS) represents circulation variability affecting Tianshan precipitation in winter. The enhanced meridional features of the EATL/WRUS pattern after 1988 lead to enhanced water vapor entering the Tianshan from low latitude oceanic regions (Guan et al., 2021a). This is further corroborated by the results in this study presented in Figure 5 and Figure 8 that the dominating moisture sources of precipitation are mainly West Asia and Indian Ocean during winter for the Western Tianshan. Warm conveyor belts embedded ahead of the trough axis of extra-tropical cyclones transport water vapor from the lower latitudes poleward (Boutle et al., 2011). Hence, up to 70% of precipitation extremes can be associated with extra-tropical cyclones or warm conveyor belts that advect moisture from West Asia and the Indian Ocean towards Western Tianshan (Pfahl et al., 2014). However, it is worth noting that according to our results (Ta-

ble 1), the significantly positive correlation between winter precipitation and moisture from West Asia and the Indian Ocean exists only in the Western Tianshan and Central Tianshan, which implies that the EATL/WRUS pattern mainly affects the west of the Tianshan Mountains where precipitation is concentrated during winter. In addition, Oh et al. (2017) found that in winter, when EATL/WRUS have the same phase combined with the Western Pacific teleconnections (WP), strong southeasterly wind anomalies deliver warm air to be transported from the tropics to East Asia. As seen from Figure (14), positive northward anomalous moisture transport from the low-latitude sub-tropics to East Asia exists in the synthesis of extreme winter precipitation months for the Western and Central Tianshan. The water vapor can be conveyed to Mongolia as well as to Siberia, which is also reflected in the significant positive correlation between winter precipitation in Western Tianshan and evaporative moisture uptake from East and South Asia, and between winter precipitation in the Central Tianshan and evaporative moisture coming from Siberia (Table 1). In summer, the Scandinavia pattern (SCAND) is strongly and negatively correlated with precipitation in Western Tianshan (Guan et al., 2021b). A strong pressure gradient enhances airflow to the Tianshan Mountains due to a persistent anticyclone over the Ural Mountains combined with the Central Asian cyclone east of the Caspian Sea (Guan et al., 2021b; Yang & He, 2003). The strong easterly flow reduces the moisture carried from Europe during extreme summer precipitation months in the Western Tianshan (15 (a)), which is an expression of the negative correlation between the summer precipitation in the Western Tianshan and the moisture contribution from Europe (Table 1). East Asia-Pacific (EAP) is another important teleconnection pattern affecting Tianshan precipitation (Guan et al., 2021a). The enhanced flux of water vapour during 1985-2004 occurred westward from East Asia to the Tianshan Mountains related to the EAP pattern. Our findings also confirm the influence of East and South Asia on Tianshan precipitation, with an emphasis on the contribution to Eastern Tianshan. During extreme summer precipitation in Eastern Tianshan, there appears to be an anomalous meridional moisture flux attributable to an "anticyclonic-cyclonic-anticyclonic" structure in the West Pacific off the coast of East Asia and Siberia which is very similar to the EAP pattern (Figure 15 (b)). Further, water vapour is transported westward from East Asia through China and Mongolia by a cyclone centered over Japan, which makes East and South Asia contribute 18.5% of moisture during extreme summer months. The extreme rainstorm event in July 2018 in the southeastern region of Hami (located in the Eastern Tianshan region) was caused by the westward transport of water vapor even from

527 the remote South China Sea into the Hami region (Liu et al., 2020). Consistently, Fan et  
528 al. (2022) found that the North Pacific pattern (NP) and the Pacific interdecadal Oscilla-  
529 tion (PDO) had an important impact on precipitation changes in Tianshan Mountains (the  
530 part within China) during 1979-2020, both of which indicate the influence of the Pacific  
531 Ocean on precipitation in the more eastern parts of the Tianshan Mountains. In addition,  
532 the anomalous anticyclone located in western Siberia conveys moisture from Siberia to the  
533 Eastern Tianshan, accounting for the increased moisture contribution from Siberia of 9.9%  
534 (average: 5.2%) during extreme precipitation in Eastern Tianshan.

535 However, it also becomes clear from the results of the Lagrangian analysis that Cen-  
536 tral Asia, including the Tianshan itself, is the main moisture source of precipitation for  
537 the Tianshan in all seasons, especially for the Northern, Central, and Eastern Tianshan.  
538 Although moisture flux from East Asia and Siberia accounts for nearly 1/3 of the extreme  
539 precipitation in the Eastern Tianshan, the share of evaporation from local evaporation as  
540 well as from Central Asia remains the dominant source even in these extreme cases (64.7%).  
541 The increase of precipitation in the Tianshan seems to be closely related to evaporation  
542 in Central Asia and from local areas. Previous studies using the Eulerian approach have  
543 shown that the Atlantic Ocean, the Caspian Sea, and the Mediterranean Sea are impor-  
544 tant sources of precipitation in the Tianshan Mountains (Li et al., 2008; Ren et al., 2016;  
545 Guan et al., 2019). Jiang, Zhou, Wang, et al. (2020) also quantified the moisture source in  
546 Central Asia using the Eulerian source-tagging method with detailed atmospheric processes  
547 and concluded that the North Atlantic Ocean could explain up to 23% of the moisture  
548 source contribution to precipitation. However, according to the applied Lagrangian ap-  
549 proach, the annual average moisture contributions of all oceanic sources to precipitation  
550 in the Western, Northern, Central, and Eastern Tianshan reaches only 9.1%, 8.1%, 5.4%,  
551 and 4.7%, respectively (Figure 8). Nevertheless, if the influence of the Northern Indian  
552 Ocean in winter is removed, then the Oceanic sources from the west including the Caspian  
553 Sea, the North Atlantic Ocean, and the Mediterranean Sea only account for 5.0%, 6.0%,  
554 2.9%, and 3.8% of the Western, Northern, Central, and Eastern Tianshan, respectively. In  
555 accordance with results from S. Yao et al. (2021) our finding demonstrates that the contri-  
556 bution of these oceans, once considered an important source of moisture, is minimal on the  
557 climate scale. Taking the North Atlantic Ocean for example, it contributes not more than  
558 5% to all Tianshan regions in all months according to the Lagrangian perspective. Only in  
559 November, it contributes nearly 5% moisture to the Northern and Eastern Tianshan guided

560 by a strong westerly component (Figure 8). These oceans certainly generate a significant  
561 amount of evaporation, which is transported by westerly winds to the Eurasian continent  
562 at mid-latitudes. However, a major part of the moisture from sea surfaces presumably is  
563 being lost to precipitation en route and possibly recycled several times by continental evap-  
564 oration and precipitation before it eventually reaches the Tianshan via moisture uptake  
565 over Central Asia. Air masses in the desert areas of Central Asia are not supplemented  
566 by sufficient local moisture and continue to move eastward bringing precipitation to the  
567 western windward slopes of the Pamir Plateau and the Northern Tianshan but are unable  
568 to affect the Eastern and Central Tianshan (S. Wang et al., 2017). S. Wang et al. (2017)  
569 therefore pointed out that precipitation in the Tianshan is more likely to be evaporation of  
570 terrestrial moisture from Europe and Central Asia rather than direct oceanic moisture from  
571 the Atlantic Ocean. More attention should be paid to local evapotranspiration variations  
572 in predicting precipitation change in Xinjiang (Peng & Zhou, 2017). Zhou et al. (2019)  
573 also concluded that Xinjiang and Central Asia are key moisture sources for extreme pre-  
574 cipitation in Xinjiang, with local contributions contributing 40% and 70% in the Ili Valley  
575 and Hami regions, respectively. These conclusions are consistent with our finding and also  
576 with the perspective that Xinjiang itself and Central Asia are the main sources of moisture  
577 contribution to precipitation in Xinjiang (S. Yao et al., 2021).

578 Central Asia has faced a significant temperature increase in recent decades, with rates  
579 of 0.36-0.42°C/10a for the period 1979-2011 and 0.34°C/10a for the period 1961-2016 in  
580 the Tianshan Mountains (Yuan-An et al., 2013; R. Hu, 2004). Rapid warming has led to a  
581 significant decrease in snow area and substantial glacier shrinkage in the Tianshan Mountains  
582 (Shangguan et al., 2015; J. Yao et al., 2022). The Central Asian regions with large glacier  
583 areas mainly show a trend of increasing runoff and increasing oasis area (Unger-Shayesteh  
584 et al., 2013; Y. Chen et al., 2016; X. Wang et al., 2020; J. Yao et al., 2022). In addition, a  
585 considerable and strong oasis expansion has occurred in Central Asia since the 1950s due to  
586 the rapid large-scale conversion of irrigation technology from traditional flood irrigation to  
587 modern drip irrigation systems (Q. Zhang et al., 2017). The oasis “irrigation effect” has a  
588 significant impact on increasing soil moisture, which in Central Asia tends to increase during  
589 1950-2015, especially in northwest China (Z. Hu et al., 2019), leading to increased surface  
590 evaporation and atmospheric water vapor content (Kueppers & Snyder, 2012; M. Zhang  
591 et al., 2019). Surface cooling from enhanced evapotranspiration in turn modifies regional  
592 wind fields and enhances convective upward movement in the lower troposphere, providing

593 moisture and favorable dynamic conditions for enhanced local rainfall (J. Yao et al., 2020).  
594 All the above contributed to the increase of local moisture in the atmosphere, which also  
595 resulted in the increase of precipitation over Central Asia and the Tianshan Mountains  
596 (M. Zhang et al., 2019). However, it is worthwhile to note that although all are located  
597 in the same arid and semi-arid zone, areas in northwest China with glaciers experience a  
598 wetting trend, while northern China and Kazakhstan located in the centre of Central Asia  
599 without glaciers suffer from increasing aridity (J. Yao et al., 2022; Gerlitz et al., 2018; Z. Hu  
600 et al., 2017; Sorg et al., 2012). Peng and Zhou (2017) stated that the increasing trend  
601 of precipitation over northwest China is dominated by the thermodynamic component in  
602 association with changes in specific humidity, which is more important than the dynamic  
603 component due to changes in atmospheric circulation. Based on these facts, we hypothesize  
604 that the melting and retreat of the Tianshan glaciers and permafrost in recent decades may  
605 be contributing to increasing precipitation around the Tianshan and northwest China, as this  
606 mechanism, may locally to regionally provide additional moisture, leading to interdecadal  
607 change from “warm-dry” to “warm-wet” conditions. Thus, the rapid melting of glaciers  
608 caused by global warming may act as a driving factor to boost runoff and increase the area  
609 of oases, which leads to an increase in local water vapour from evaporation and eventually  
610 precipitation. This may act in terms of a positive feedback loop by increasing precipitation  
611 and in turn enhancing the oasis area and local evaporation (J. Yao et al., 2022). Under  
612 the long-term effect of this positive cycle, precipitation might increase in the Tianshan and  
613 Central Asia. However, the volume of mountain glacier ice is limited. Moreover, glacier  
614 retreat under progressing climate warming is irreversible on time scales of tens to hundreds  
615 of years. Thus, the “wetting” in Central Asia, including the Tianshan Mountains, is likely  
616 to be only a short-term fluctuation of the drying trend at the centennial-millennial scales  
617 (Jiang, Zhou, Chen, & Zhang, 2020; He et al., 2021). However, any quantitative analysis  
618 of the local water cycle including the contribution of meltwater from Tianshan glaciers lies  
619 beyond the scope and options of the current study.

620 Precipitation has not easily reproduced accurately in the Tianshan Mountains due to the  
621 scarcity of weather stations, especially at high altitudes. Although the correlation coefficient  
622 between precipitation in the Tianshan Mountains based on GPCC precipitation data and  
623 ERA-Interim data reaches 0.84 ( $p \leq 0.01$ ), the temporal trends of precipitation still vary  
624 from region to region and even show opposite sign between GPCC and ERA-Interim data.  
625 In addition to the uncertainty of both the measured and spatially interpolated precipitation

626 data, and precipitation derived from numerical weather forecast reanalysis, the Lagrangian  
627 precipitation estimation in this study has its own limitations. As can be seen in (Figure  
628 2), although the Lagrangian estimated precipitation captures the main characteristics of  
629 precipitation in the Tianshan Mountains, its value is larger than both the ERA-Interim  
630 and GPCC datasets. Such overestimation has previously been reported in studies using the  
631 Lagrangian method (Sodemann et al., 2008; Stohl & James, 2004; James et al., 2004; S. Yao  
632 et al., 2021). The main reason for the positive bias of estimated precipitation is due to the  
633 assumption that the decrease in  $\Delta q$  is completely counted as precipitation at the target  
634 location during the last 6 h before the starting point, rather than being allocated over the  
635 region that was traversed by the air mass during that final 6 h of the trajectory. Meanwhile,  
636 processes such as convection and the formation of ice crystals and water droplets during  
637 the cloud condensation process are neglected in the Lagrangian approach. In addition, as  
638 we mentioned in Section 3.1, all attributed moisture sources are considered as the sources  
639 of precipitation in Tianshan Mountains in this study. This follows the notion of Sodemann  
640 and Zubler (2010) who stated that if the distribution of moisture sources above and within  
641 the PBL performs similarly, then the moisture sources in the study area are not likely to  
642 differ significantly within and above the PBL. However, since only moisture uptake within  
643 the PBL can be directly linked to evaporation from the underlying surface, it is still possible  
644 that the absolute value and extent of moisture sources affecting precipitation in the Tianshan  
645 Mountains are overestimated to some degree.

## 646 **5 Conclusion**

647 In this study a Lagrangian method is used to identify the moisture source patterns of  
648 precipitation over the Tianshan Mountains and to analyse the quantitative contributions of  
649 the main moisture source areas during 1979-2017. All attributed moisture sources (evap-  
650 oration within the PBL plus evaporation above the PBL) have been considered, with the  
651 highest evaporation contribution area mainly concentrated in Central Asia and locally in  
652 the Tianshan itself. The moisture source contributions vary both seasonally and between  
653 different sub-regions of the Tianshan Mountains. More long-range moisture transport exists  
654 during winter (November - March) due to the enhanced westerlies, especially for the West-  
655 ern Tianshan, while the moisture source distribution extends more northward and eastward  
656 in summer (April - October).

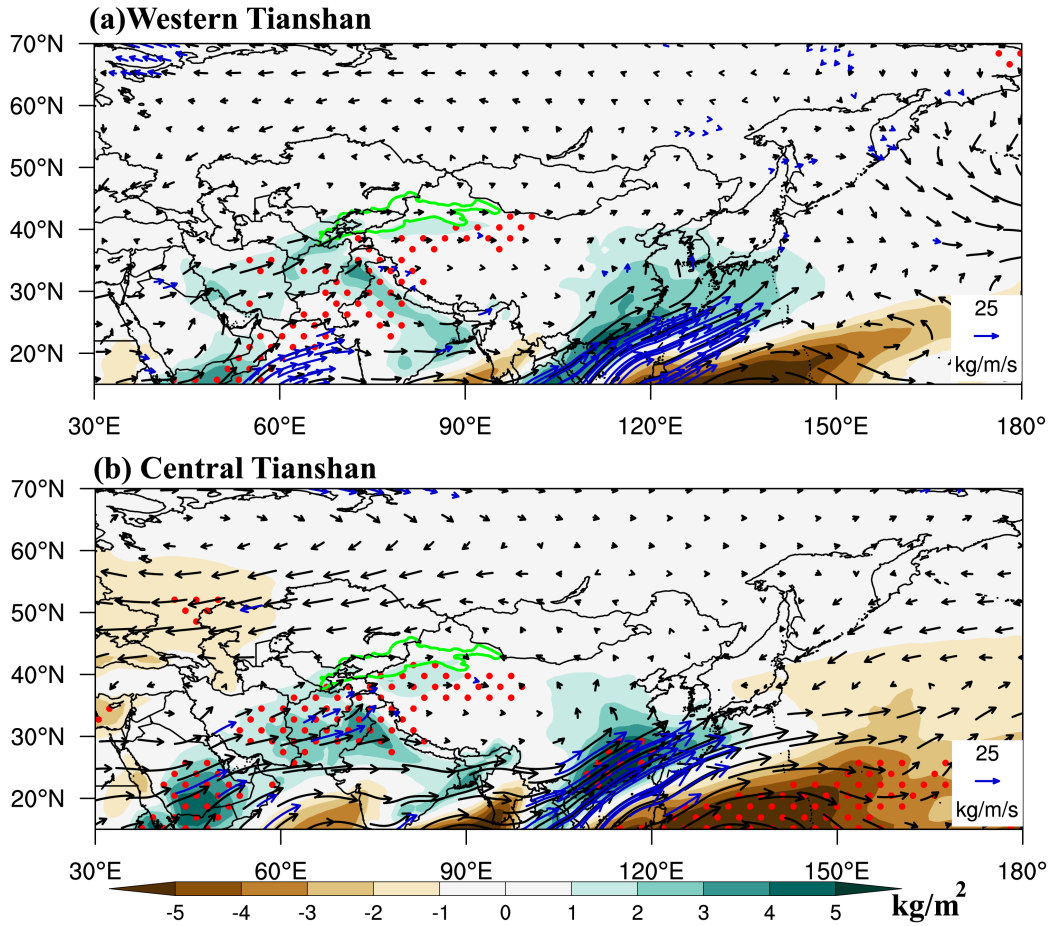


**Figure 14.** Anomalies of water vapour flux (vector in kg/m/s) and total precipitable water vapour content (PWC in kg/m<sup>2</sup>) during extreme winter precipitation in (a) Western Tianshan; (b) Central Tianshan. Areas with red dots and the blue arrows indicate the anomalies of PWC and water vapour flux significant at the 95% confidence level, respectively.

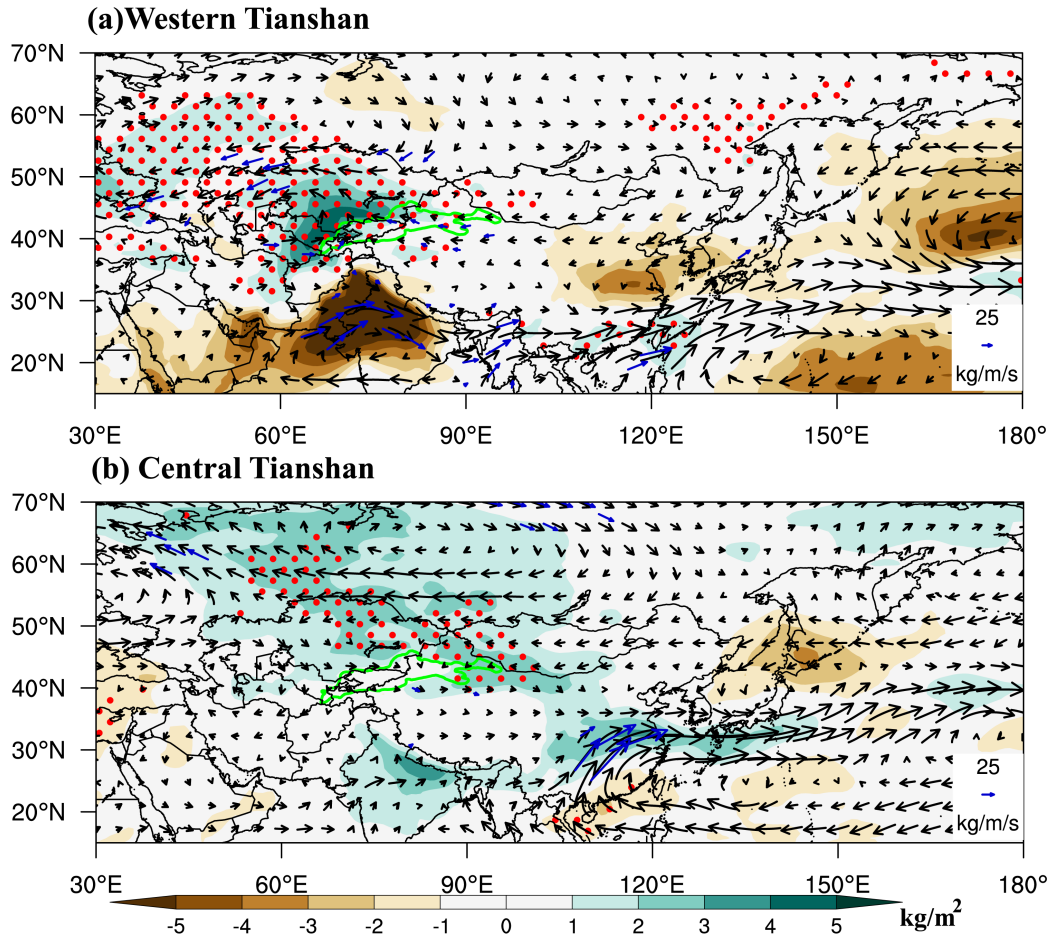


**Figure 15.** Anomalies of water vapour flux (vector in kg/m/s) and total precipitable water vapour content (PWC in kg/m<sup>2</sup>) during extreme summer precipitation in (a) Western Tianshan; (b) Eastern Tianshan. Areas with red dots and the blue arrows indicate the anomalies of PWC and water vapour flux significant at the 95% confidence level, respectively.

657 Continental sources provide about 93.2% of the precipitation in the Tianshan. Specif-  
658 ically, continental sources contributed 90.9%, 91.9%, 94.6%, and 95.3% of the moisture to  
659 the Western, Northern, Central, and Eastern Tianshan, respectively. Among the continental  
660 sources, Central Asia plays a leading role in providing moisture for all sub-regions of the  
661 Tianshan Mountains. Excluding the indirect effect of moisture transport from the Ocean  
662 to nearby terrestrial land on precipitation in the Tianshan Mountains, the annual average  
663 moisture contribution directly from all Oceanic sources to precipitation in the Western,  
664 Northern, Central, and Eastern Tianshan reach 9.1%, 8.1%, 5.4%, and 4.7%, respectively.

665 For the Western Tianshan, the main contributors are Central Asia (31.8%) and West  
666 Asia (29.8%). These shares of these two moisture sources change between seasons. Moisture  
667 in summer months is advected mainly from Central Asia, with mean contributions of 41.0%,  
668 while in winter months it comes mainly from West Asia (45.7%). In addition, Tianshan  
669 itself supplies 17.2% of moisture contribution and the Indian Ocean provides 7.2% of the  
670 moisture to precipitation in winter for Western Tianshan. Central Asia and Tianshan itself  
671 explain 37.1% and 22.5% of the moisture contribution, respectively, and are identified as  
672 the main moisture source in the Northern Tianshan. Slightly further remote areas of West  
673 Asia and continental Europe also account for 19.5% and 7.3% of the contribution. For  
674 the precipitation of Central and Eastern Tianshan, we also identify local evaporation and  
675 Central Asia as the dominant moisture source, providing 66.8% and 69.9% of the moisture,  
676 respectively. It is followed by West Asia, which supplies 18.0% and 10.4% of moisture,  
677 respectively. In addition, 7.7% and 5.2% of moisture for precipitation in Eastern Tianshan  
678 originate from East and South Asia and Siberia in summer, which is different from all other  
679 Tianshan sub-regions.

680 From 1979-2017, there is no significant annual variation in the contribution of most  
681 moisture sources, including the predominant moisture source, Central Asia, for Western,  
682 Northern, and Central Tianshan. However, the contribution of moisture originating from  
683 Europe to precipitation for Central Tianshan and Eastern Tianshan all show a significant  
684 decreasing trend in summer with linear trends of -0.06mm/10a and -0.03mm/10a, respec-  
685 tively. The contribution of the North Atlantic Ocean to precipitation for Northern, Cen-  
686 tral, and Eastern Tianshan in summer also shows a decreasing trend with linear trends  
687 of -0.05mm/10a, -0.02mm/10a, and -0.01mm/10a, respectively, though its relative direct  
688 contribution to the Tianshan Mountains is limited anyway.

689 During extreme winter precipitation months, the largest increase of moisture in the  
690 Western Tianshan derives from West Asia (contribution in 54.1%). Apart from the evapo-  
691 ration from local and Central Asia, the gain of moisture from East and South Asia as well  
692 as Siberia in the Eastern Tianshan is obvious. Europe is also an important contributor to  
693 extreme precipitation months in the Northern Tianshan while for the Central Tianshan, on  
694 the other hand, the increase in local evaporation has the greatest impact on its extreme  
695 winter precipitation. Extreme summer precipitation months in the Tianshan Mountains  
696 are mainly caused by enhanced local evaporation and enhanced moisture flux from Central  
697 Asia. The Eastern Tianshan differs from other Tianshan regions in that moisture contribu-  
698 tion from East and South Asia as well as Siberia increases significantly during periods with  
699 extreme precipitation.

## 700 **Acknowledgments**

701  
702 We would like to thank the China Scholarship Council (CSC) for their support to  
703 Xuefeng Guan who is pursuing her Ph.D. degree at the Humboldt-Universität zu Berlin. We  
704 are also grateful to Tobias Sauter (Geography Department, Humboldt-Universität zu Berlin)  
705 and Junqiang Yao (Institute of Desert Meteorology, China Meteorological Administration)  
706 for valuable and fruitful discussions on earlier versions of the manuscript. We acknowledge  
707 support by the Open Access Publication Fund of the Humboldt-Universität zu Berlin.

708 Data Availability Statement: The ERA-Interim reanalysis data can be retrieved from  
709 the European Center for Medium-Range Weather Forecasts (<https://www.ecmwf.int/en/forecasts/datasets/reanalysis-datasets/era-interim>). The GPCC precipitation  
710 Data can be downloaded from Global Precipitation Climatology Centre (<https://www.dwd.de/EN/ourservices/gpcc/gpcc.html>).

713 We are pleased to make available to researchers interested in the monthly moisture  
714 sources of the Tianshan Mountains (1979-2017) obtained from the Lagrangian diagnostics.  
715 Xuefeng Guan, Lukas Langhamer, & Christoph Schneider. (2022). Moisture sources data  
716 of Tianshan Mountains [Data set]. Zenodo. <https://doi.org/10.5281/zenodo.6320458>

## 717 **References**

718 Aizen, V. B., Aizen, E. M., & Melack, J. M. (1995). Climate, snow cover, glaciers, and runoff

- 719 in the tien shan, central asia 1. *JAWRA Journal of the American Water Resources*  
720 *Association*, 31(6), 1113–1129.
- 721 Aizen, V. B., Aizen, E. M., Melack, J. M., & Dozier, J. (1997). Climatic and hydrologic  
722 changes in the tien shan, central asia. *Journal of Climate*, 10(6), 1393–1404.
- 723 Aizen, V. B., Kuzmichenok, V. A., Surazakov, A. B., & Aizen, E. M. (2006). Glacier changes  
724 in the central and northern tien shan during the last 140 years based on surface and  
725 remote-sensing data. *Annals of Glaciology*, 43, 202–213.
- 726 Armstrong, R. L., Rittger, K., Brodzik, M. J., Racoviteanu, A., Barrett, A. P., Khalsa,  
727 S.-J. S., ... others (2019). Runoff from glacier ice and seasonal snow in high asia:  
728 separating melt water sources in river flow. *Regional Environmental Change*, 19(5),  
729 1249–1261.
- 730 Bekturganov, Z., Tussupova, K., Berndtsson, R., Sharapatova, N., Aryngazin, K., &  
731 Zhanasova, M. (2016). Water related health problems in central asia—a review.  
732 *Water*, 8(6), 219.
- 733 Berrisford, P., Källberg, P., Kobayashi, S., Dee, D., Uppala, S., Simmons, A., ... Sato, H.  
734 (2011). Atmospheric conservation properties in era-interim. *Quarterly Journal of the*  
735 *Royal Meteorological Society*, 137(659), 1381–1399.
- 736 Bothe, O., Fraedrich, K., & Zhu, X. (2012). Precipitation climate of central asia and  
737 the large-scale atmospheric circulation. *Theoretical and applied climatology*, 108(3),  
738 345–354.
- 739 Boutle, I. A., Belcher, S. E., & Plant, R. S. (2011). Moisture transport in midlatitude  
740 cyclones: Cyclone moisture transport. , 137(655), 360–373. Retrieved 2022-02-15, from  
741 <https://onlinelibrary.wiley.com/doi/10.1002/qj.783> doi: 10.1002/qj.783
- 742 Chen, S., Gan, T. Y., Tan, X., Shao, D., & Zhu, J. (2019). Assessment of cfsr, era-interim,  
743 jra-55, merra-2, ncep-2 reanalysis data for drought analysis over china. *Climate Dy-*  
744 *namics*, 53(1), 737–757.
- 745 Chen, Y., Li, W., Deng, H., Fang, G., & Li, Z. (2016). Changes in central asia’s water  
746 tower: past, present and future. *Scientific reports*, 6(1), 1–12.
- 747 Dee, D. P., Uppala, S. M., Simmons, A. J., Berrisford, P., Poli, P., Kobayashi, S., ...  
748 others (2011). The era-interim reanalysis: Configuration and performance of the data  
749 assimilation system. *Quarterly Journal of the royal meteorological society*, 137(656),  
750 553–597.
- 751 Durán-Quesada, A. M., Gimeno, L., Amador, J., & Nieto, R. (2010). Moisture sources

- 752 for central america: Identification of moisture sources using a lagrangian analysis  
753 technique. *Journal of Geophysical Research: Atmospheres*, 115(D5).
- 754 Fan, M., Xu, J., Li, D., & Chen, Y. (2022). Response of precipitation in tianshan to global  
755 climate change based on the berkeley earth and era5 reanalysis products. *Remote*  
756 *Sensing*, 14(3), 519.
- 757 Farinotti, D., Longuevergne, L., Moholdt, G., Duethmann, D., Mölg, T., Bolch, T., ...  
758 Güntner, A. (2015). Substantial glacier mass loss in the tien shan over the past 50  
759 years. *Nature Geoscience*, 8(9), 716–722.
- 760 Feng, F., Li, Z., Zhang, M., Jin, S., & Dong, Z. (2013). Deuterium and oxygen 18 in precip-  
761 itation and atmospheric moisture in the upper urumqi river basin, eastern tianshan  
762 mountains. *Environmental Earth Sciences*, 68(4), 1199–1209.
- 763 Freedman, D., Pisani, R., & Purves, R. (2007). Statistics (international student edition).  
764 *Pisani, R. Purves, 4th edn. WW Norton & Company, New York.*
- 765 Gao, Y., Xiao, L., Chen, D., Xu, J., & Zhang, H. (2018). Comparison between past and  
766 future extreme precipitations simulated by global and regional climate models over  
767 the tibetan plateau. *International Journal of Climatology*, 38(3), 1285–1297.
- 768 Gerlitz, L., Conrad, O., Thomas, A., & Böhner, J. (2014). Warming patterns over the  
769 tibetan plateau and adjacent lowlands derived from elevation-and bias-corrected era-  
770 interim data. *Climate research*, 58(3), 235–246.
- 771 Gerlitz, L., Steirou, E., Schneider, C., Moron, V., Vorogushyn, S., & Merz, B. (2018).  
772 Variability of the cold season climate in central asia. part i: weather types and their  
773 tropical and extratropical drivers. *Journal of climate*, 31(18), 7185–7207.
- 774 Gimeno, L., Nieto, R., Trigo, R. M., Vicente-Serrano, S. M., & López-Moreno, J. I. (2010).  
775 Where does the iberian peninsula moisture come from? an answer based on a la-  
776 grangian approach. *Journal of Hydrometeorology*, 11(2), 421–436.
- 777 Gimeno, L., Stohl, A., Trigo, R. M., Dominguez, F., Yoshimura, K., Yu, L., ... Nieto,  
778 R. (2012). Oceanic and terrestrial sources of continental precipitation. *Reviews of*  
779 *Geophysics*, 50(4).
- 780 Guan, X., Yang, L., Zhang, Y., & Li, J. (2019). Spatial distribution, temporal variation,  
781 and transport characteristics of atmospheric water vapor over central asia and the arid  
782 region of china. *Global and Planetary Change*, 172, 159–178.
- 783 Guan, X., Yao, J., & Schneider, C. (2021a). Variability of the precipitation over the tian-  
784 shan mountains, central asia. part ii: Multi-decadal precipitation trends and their

- 785 association with atmospheric circulation in both the winter and summer seasons. *In-*  
786 *ternational Journal of Climatology*.
- 787 Guan, X., Yao, J., & Schneider, C. (2021b). Variability of the precipitation over the tianshan  
788 mountains, central asia. part i: Linear and nonlinear trends of the annual and seasonal  
789 precipitation. *International Journal of Climatology*.
- 790 Guo, Y., Xu, X., Chen, W., Wei, F., & Chen, A. (2014). Heat source over ‘fishtail’ type  
791 topography effects on tianshan mountain regions precipitation systems and water re-  
792 sources. *Plateau Meteorology*, *33*(5), 1363–1373.
- 793 Hamm, A., Arndt, A., Kolbe, C., Wang, X., Thies, B., Boyko, O., . . . Schneider, C. (2020).  
794 Intercomparison of gridded precipitation datasets over a sub-region of the central  
795 himalaya and the southwestern tibetan plateau. *Water*, *12*(11), 3271.
- 796 He, H., Luo, G., Cai, P., Hamdi, R., Termonia, P., De Maeyer, P., . . . Li, J. (2021).  
797 Assessment of climate change in central asia from 1980 to 2100 using the köppen-  
798 geiger climate classification. *Atmosphere*, *12*(1), 123.
- 799 Hu, R. (2004). Physical geography of the tianshan mountains in china. *China Environmental*  
800 *Science Press, Beijing*, 264–273.
- 801 Hu, Z., Chen, X., Chen, D., Li, J., Wang, S., Zhou, Q., . . . Guo, M. (2019). “dry gets drier,  
802 wet gets wetter”: A case study over the arid regions of central asia. *International*  
803 *Journal of Climatology*, *39*(2), 1072–1091.
- 804 Hu, Z., Hu, Q., Zhang, C., Chen, X., & Li, Q. (2016). Evaluation of reanalysis, spatially in-  
805 terpolated and satellite remotely sensed precipitation data sets in central asia. *Journal*  
806 *of Geophysical Research: Atmospheres*, *121*(10), 5648–5663.
- 807 Hu, Z., Zhang, C., Hu, Q., & Tian, H. (2014). Temperature changes in central asia from  
808 1979 to 2011 based on multiple datasets. *Journal of Climate*, *27*(3), 1143–1167.
- 809 Hu, Z., Zhou, Q., Chen, X., Qian, C., Wang, S., & Li, J. (2017). Variations and changes  
810 of annual precipitation in central asia over the last century. *International Journal of*  
811 *Climatology*, *37*, 157–170.
- 812 Hua, L., Zhong, L., & Ma, Z. (2017). Decadal transition of moisture sources and transport  
813 in northwestern china during summer from 1982 to 2010. *Journal of Geophysical*  
814 *Research: Atmospheres*, *122*(23), 12–522.
- 815 Huang, W., Chang, S.-Q., Xie, C.-L., & Zhang, Z.-P. (2017). Moisture sources of extreme  
816 summer precipitation events in north xinjiang and their relationship with atmospheric  
817 circulation. *Advances in Climate Change Research*, *8*(1), 12–17.

- 818 Huang, W., Chen, F., Feng, S., Chen, J., & Zhang, X. (2013). Interannual precipitation  
819 variations in the mid-latitude asia and their association with large-scale atmospheric  
820 circulation. *Chinese Science Bulletin*, *58*(32), 3962–3968.
- 821 Huang, W., Chen, J., Zhang, X., Feng, S., & Chen, F. (2015). Definition of the core zone  
822 of the “westerlies-dominated climatic regime”, and its controlling factors during the  
823 instrumental period. *Science China Earth Sciences*, *58*(5), 676–684.
- 824 Immerzeel, W., & Bierkens, M. (2012). Asia’s water balance. *Nature Geoscience*, *5*(12),  
825 841–842.
- 826 James, P., Stohl, A., Spichtinger, N., Eckhardt, S., & Forster, C. (2004). Climatological  
827 aspects of the extreme european rainfall of august 2002 and a trajectory method  
828 for estimating the associated evaporative source regions. *Natural Hazards and Earth  
829 System Sciences*, *4*(5/6), 733–746.
- 830 Jiang, J., Zhou, T., Chen, X., & Zhang, L. (2020). Future changes in precipitation over cen-  
831 tral asia based on cmip6 projections. *Environmental Research Letters*, *15*(5), 054009.
- 832 Jiang, J., Zhou, T., Wang, H., Qian, Y., Noone, D., & Man, W. (2020). Tracking moisture  
833 sources of precipitation over central asia: A study based on the water-source-tagging  
834 method. *Journal of Climate*, *33*(23), 10339–10355.
- 835 Kendall, M. (1975). *Rank correlation measures (london: Charles griffin)*.
- 836 Knippertz, P., & Wernli, H. (2010). A lagrangian climatology of tropical moisture exports  
837 to the northern hemispheric extratropics. *Journal of Climate*, *23*(4), 987–1003.
- 838 Kueppers, L. M., & Snyder, M. A. (2012). Influence of irrigated agriculture on diurnal sur-  
839 face energy and water fluxes, surface climate, and atmospheric circulation in california.  
840 *Climate Dynamics*, *38*(5), 1017–1029.
- 841 Langhamer, L., Dublyansky, Y., & Schneider, C. (2021). Spatial and temporal planetary  
842 boundary layer moisture-source variability of crimean peninsula precipitation. *Earth  
843 and Space Science*, e2021EA001727.
- 844 Langhamer, L., Sauter, T., & Mayr, G. J. (2018). Lagrangian detection of moisture sources  
845 for the southern patagonia icefield (1979–2017). *Frontiers in Earth Science*, 219.
- 846 Lemenkova, P. (2013). Current problems of water supply and usage in central asia, tian  
847 shan basin. In *Environmental and climate technologies. proceedings of 54th interna-  
848 tional scientific conference (riga technical university, institute of energy systems and  
849 environment)*.
- 850 Li, W., Wang, K., Fu, S., & Jiang, H. (2008). The interrelationship between regional

- 851 westerly index and the water vapor budget in northwest china. *Journal of Glaciology*  
852 *and Geocryology*, 30(1), 28–34.
- 853 Liu, J., Liu, F., Tuoliewubieke, D., & Yang, L. (2020). Analysis of the water vapour  
854 transport and accumulation mechanism during the “7.31” extreme rainstorm event in  
855 the southeastern hami area, china. *Meteorological Applications*, 27(4), e1933.
- 856 Liu, J., & Zhang, W. (2017). Long term spatio-temporal analyses of snow cover in cen-  
857 tral asia using era-interim and modis products. In *Iop conference series: Earth and*  
858 *environmental science* (Vol. 57, p. 012033).
- 859 Mann, H. (1945). *Non-parametric tests against trend. econometria*. Chicago.
- 860 Mariotti, A. (2007). How enso impacts precipitation in southwest central asia. *Geophysical*  
861 *research letters*, 34(16).
- 862 Nieto, R., Gimeno, L., & Trigo, R. M. (2006). A lagrangian identification of major sources  
863 of sahel moisture. *Geophysical Research Letters*, 33(18).
- 864 Oh, H., Jhun, J.-G., Ha, K.-J., & Seo, K.-H. (2017). Combined effect of the east atlantic/west  
865 russia and western pacific teleconnections on the east asian winter monsoon. *Asia-*  
866 *Pacific Journal of Atmospheric Sciences*, 53(2), 273–285.
- 867 Ososkova, T., Gorelkin, N., & Chub, V. (2000). Water resources of central asia and adapta-  
868 tion measures for climate change. *Environmental monitoring and assessment*, 61(1),  
869 161–166.
- 870 Owens, R., & Hewson, T. (2018). Ecmwf forecast user guide. *Reading: ECMWF*, 10,  
871 m1cs7h.
- 872 Peng, D., & Zhou, T. (2017). Why was the arid and semiarid northwest china getting wetter  
873 in the recent decades? *Journal of Geophysical Research: Atmospheres*, 122(17), 9060–  
874 9075.
- 875 Pfahl, S., Madonna, E., Boettcher, M., Joos, H., & Wernli, H. (2014). Warm conveyor belts  
876 in the ERA-interim dataset (1979–2010). part II: Moisture origin and relevance for  
877 precipitation. , 27(1), 27–40. Retrieved 2022-02-15, from [http://journals.ametsoc](http://journals.ametsoc.org/doi/10.1175/JCLI-D-13-00223.1)  
878 [.org/doi/10.1175/JCLI-D-13-00223.1](http://journals.ametsoc.org/doi/10.1175/JCLI-D-13-00223.1) doi: 10.1175/JCLI-D-13-00223.1
- 879 Ramos, A. M., Nieto, R., Tomé, R., Gimeno, L., Trigo, R. M., Liberato, M. L., & Lavers,  
880 D. A. (2016). Atmospheric rivers moisture sources from a lagrangian perspective.  
881 *Earth System Dynamics*, 7(2), 371–384.
- 882 Ren, G., Yuan, Y., Liu, Y., Ren, Y., Wang, T., & Ren, X. (2016). Changes in precipitation  
883 over northwest china. *Arid zone research*, 33(1), 1–19.

- 884 Schiemann, R., Lüthi, D., Vidale, P. L., & Schär, C. (2008). The precipitation climate  
885 of central asia—intercomparison of observational and numerical data sources in a  
886 remote semiarid region. *International Journal of Climatology: A Journal of the Royal  
887 Meteorological Society*, *28*(3), 295–314.
- 888 Schneider, U., Becker, A., Finger, P., Meyer-Christoffer, A., & Ziese, M. (2018). Gpcc full  
889 data monthly product version 2018 at 0.25°: Monthly land-surface precipitation from  
890 rain-gauges built on gts-based and historical data. *GPCC: Offenbach, Germany*.
- 891 Schuster, L., Maussion, F., Langhamer, L., & Moseley, G. E. (2021). Lagrangian detection  
892 of precipitation moisture sources for an arid region in northeast greenland: relations  
893 to the north atlantic oscillation, sea ice cover, and temporal trends from 1979 to 2017.  
894 *Weather and Climate Dynamics*, *2*(1), 1–17.
- 895 Shangguan, D. H., Bolch, T., Ding, Y., Kröhnert, M., Pieczonka, T., Wetzol, H.-U., & Liu,  
896 S. (2015). Mass changes of southern and northern inylchek glacier, central tian shan,  
897 kyrgyzstan, during 1975 and 2007 derived from remote sensing data. *The Cryosphere*,  
898 *9*(2), 703–717.
- 899 Sodemann, H., Schwierz, C., & Wernli, H. (2008). Interannual variability of greenland winter  
900 precipitation sources: Lagrangian moisture diagnostic and north atlantic oscillation  
901 influence. *Journal of Geophysical Research: Atmospheres*, *113*(D3).
- 902 Sodemann, H., & Zubler, E. (2010). Seasonal and inter-annual variability of the moisture  
903 sources for alpine precipitation during 1995–2002. *International Journal of Climatol-  
904 ogy: A Journal of the Royal Meteorological Society*, *30*(7), 947–961.
- 905 Song, M.-y., Li, Z.-q., Xia, D.-s., Jin, S., & Zhang, X. (2019). Isotopic evidence for the  
906 moisture origin and influencing factors at urumqi glacier no. 1 in upstream urumqi  
907 river basin, eastern tianshan mountains. *Journal of Mountain Science*, *16*(8), 1802–  
908 1815.
- 909 Sorg, A., Bolch, T., Stoffel, M., Solomina, O., & Beniston, M. (2012). Climate change  
910 impacts on glaciers and runoff in tien shan (central asia). *Nature Climate Change*,  
911 *2*(10), 725–731.
- 912 Sprenger, M., & Wernli, H. (2015). The lagranto lagrangian analysis tool—version 2.0.  
913 *Geoscientific Model Development*, *8*(8), 2569–2586.
- 914 Stohl, A., & James, P. (2004). A lagrangian analysis of the atmospheric branch of the global  
915 water cycle. part i: Method description, validation, and demonstration for the august  
916 2002 flooding in central europe. *Journal of Hydrometeorology*, *5*(4), 656–678.

- 917 Sun, B., & Wang, H. (2014). Moisture sources of semiarid grassland in china using the  
918 lagrangian particle model flexpart. *Journal of Climate*, *27*(6), 2457–2474.
- 919 Unger-Shayesteh, K., Vorogushyn, S., Farinotti, D., Gafurov, A., Duethmann, D., Mandy-  
920 chev, A., & Merz, B. (2013). What do we know about past changes in the water cycle  
921 of central asian headwaters? a review. *Global and Planetary Change*, *110*, 4–25.
- 922 Wang, S., Zhang, M., Crawford, J., Hughes, C. E., Du, M., & Liu, X. (2017). The effect of  
923 moisture source and synoptic conditions on precipitation isotopes in arid central asia.  
924 *Journal of Geophysical Research: Atmospheres*, *122*(5), 2667–2682.
- 925 Wang, S., Zhang, M., Sun, M., Wang, B., & Li, X. (2013). Changes in precipitation extremes  
926 in alpine areas of the chinese tianshan mountains, central asia, 1961–2011. *Quaternary*  
927 *International*, *311*, 97–107.
- 928 Wang, W., Li, H., Wang, J., & Hao, X. (2020). Water vapor from western eurasia promotes  
929 precipitation during the snow season in northern xinjiang, a typical arid region in  
930 central asia. *Water*, *12*(1), 141.
- 931 Wang, X., Yang, T., Xu, C.-Y., Xiong, L., Shi, P., & Li, Z. (2020). The response of  
932 runoff components and glacier mass balance to climate change for a glaciated high-  
933 mountainous catchment in the tianshan mountains. *Natural Hazards*, *104*(2), 1239–  
934 1258.
- 935 Weigel, A. P., Chow, F. K., & Rotach, M. W. (2007). The effect of mountainous topography  
936 on moisture exchange between the “surface” and the free atmosphere. *Boundary-Layer*  
937 *Meteorology*, *125*(2), 227–244.
- 938 Wernli, H., & Davies, H. C. (1997). A lagrangian-based analysis of extratropical cyclones.  
939 i: The method and some applications. *Quarterly Journal of the Royal Meteorological*  
940 *Society*, *123*(538), 467–489.
- 941 Winschall, A., Pfahl, S., Sodemann, H., & Wernli, H. (2014). Comparison of eulerian and  
942 lagrangian moisture source diagnostics—the flood event in eastern europe in may 2010.  
943 *Atmospheric Chemistry and Physics*, *14*(13), 6605–6619.
- 944 Xenarios, S., Gafurov, A., Schmidt-Vogt, D., Sehring, J., Manandhar, S., Hergarten, C., . . .  
945 Foggin, M. (2019). Climate change and adaptation of mountain societies in central  
946 asia: uncertainties, knowledge gaps, and data constraints. *Regional Environmental*  
947 *Change*, *19*(5), 1339–1352.
- 948 Xingang, D., Weijing, L., Zhuguo, M., & Ping, W. (2007). Water-vapor source shift of  
949 xinjiang region during the recent twenty years. *Progress in natural science*, *17*(5),

- 950 569–575.
- 951 Yang, Q., & He, Q. (2003). Climate change in the western tianshan mountainous and  
952 climate effect of oasis. *Journal of Glaciology and Geocryology*, *3*.
- 953 Yao, J., Chen, Y., Guan, X., Zhao, Y., Chen, J., & Mao, W. (2022). Recent climate and  
954 hydrological changes in a mountain–basin system in xinjiang, china. *Earth-Science*  
955 *Reviews*, 103957.
- 956 Yao, J., Chen, Y., Zhao, Y., Guan, X., Mao, W., & Yang, L. (2020). Climatic and associated  
957 atmospheric water cycle changes over the xinjiang, china. *Journal of Hydrology*, *585*,  
958 124823.
- 959 Yao, J., Liu, X., & Hu, W. (2021). Stable isotope compositions of precipitation over central  
960 asia. *PeerJ*, *9*, e11312.
- 961 Yao, S., Jiang, D., & Zhang, Z. (2021). Lagrangian simulations of moisture sources for  
962 chinese xinjiang precipitation during 1979–2018. *International Journal of Climatology*,  
963 *41*, E216–E232.
- 964 Yatagai, A., Kamiguchi, K., Arakawa, O., Hamada, A., Yasutomi, N., & Kitoh, A. (2012).  
965 Aphrodite: Constructing a long-term daily gridded precipitation dataset for asia based  
966 on a dense network of rain gauges. *Bulletin of the American Meteorological Society*,  
967 *93*(9), 1401–1415.
- 968 Yuan, Y., He, Q., & Yu, S. (2004). Feature of annual precipitation change in tianshan  
969 mountain area for the recent 40 years and comparison with those in the south and  
970 north xinjiang. *Scientia Meteorological Sinica*, *24*, 220–226.
- 971 Yuan-An, J., Ying, C., Yi-Zhou, Z., Peng-Xiang, C., Xing-Jie, Y., Jing, F., & Su-Qin, B.  
972 (2013). Analysis on changes of basic climatic elements and extreme events in xinjiang,  
973 china during 1961–2010. *Advances in Climate Change Research*, *4*(1), 20–29.
- 974 Zeng, X., Brunke, M. A., Zhou, M., Fairall, C., Bond, N. A., & Lenschow, D. H. (2004).  
975 Marine atmospheric boundary layer height over the eastern pacific: Data analysis and  
976 model evaluation. *Journal of Climate*, *17*(21), 4159–4170.
- 977 Zhang, H., Ouyang, Z., Zheng, H., & Wang, X. (2009). Recent climate trends on the northern  
978 slopes of the tianshan mountains, xinjiang, china. *Journal of Mountain Science*, *6*(3),  
979 255–265.
- 980 Zhang, M., Luo, G., Cao, X., Hamdi, R., Li, T., Cai, P., ... He, H. (2019). Numerical  
981 simulation of the irrigation effects on surface fluxes and local climate in typical  
982 mountain-oasis-desert systems in the central asia arid area. *Journal of Geophysical*

983 *Research: Atmospheres*, 124(23), 12485–12506.

984 Zhang, Q., Luo, G., Li, L., Zhang, M., Lv, N., & Wang, X. (2017). An analysis of oasis  
985 evolution based on land use and land cover change: A case study in the sangong  
986 river basin on the northern slope of the tianshan mountains. *Journal of Geographical  
987 Sciences*, 27(2), 223–239.

988 Zhao, P., Gao, L., Wei, J., Ma, M., Deng, H., Gao, J., & Chen, X. (2020). Evaluation  
989 of era-interim air temperature data over the qilian mountains of china. *Advances in  
990 Meteorology*, 2020.

991 Zhou, Y.-s., Xie, Z.-m., & Liu, X. (2019). An analysis of moisture sources of torrential  
992 rainfall events over xinjiang, china. *Journal of Hydrometeorology*, 20(10), 2109–2122.